MANGANESE DIOXIDE — A REVIEW OF A BATTERY CHEMICAL PART II. SOLID STATE AND ELECTROCHEMICAL PROPERTIES OF MANGANESE DIOXIDES

BUQUI D. DESAI*, JULIO B. FERNANDES and V. N. KAMAT DALAL

Department of Chemistry, Centre of Post-graduate Instruction and Research, 'Susheela' 18th June Road, Panaji-Goa 403 001 (India)

(Received August 6, 1984; in revised form April 10, 1985)

Summary

A literature survey indicated that the properties such as electrical conductivity, magnetic susceptibility, thermal decomposition temperature and water content influence the activity of manganese dioxides.

Infrared spectroscopy is considered as a convenient analytical tool with which to characterize the various crystal phases of the dioxides. Increasing attention has also been given to predicting the potentials of the system $(MnO_2)_{1-r}$. $MnOOH_r$ during electrochemical reduction with a view to understanding the observed discharge characteristics.

Further, attempts are being made to correlate the activity of the dioxides with their structural features.

1. Introduction

There has been a phenomenal rise over the years in the consumption of manganese dioxides for use as the active cathode material in MnO_2-based dry cells. Rechargeability of the MnO_2 cathode has greatly increased its industrial potential. In this review the electrochemistry of the dioxides is discussed with special emphasis on recent developments in the field, in particular the solid state properties.

2. Solid state properties

2.1. Electrical conductivity

Not much has been published on the electrical conductivity of manganese dioxides. A substantial part of the available literature is confined to pyrolytic β-MnO_2 and electrolytic γ-MnO_2; other MnO_2 polymorphs

*Author to whom correspondence should be addressed. Present address: Dept. of Chemistry, Goa University, Goa Medical College Complex, Bambolim-Goa 403 005, India.

0378-7753/85/$3.30

have not been studied adequately. This is probably due to the experimental difficulties involved in dealing mainly with powders instead of monocrystals [1]. Pellets of MnO_2 powder are difficult to form and conductivity studies are usually done within the press-tool. Manganese dioxide is known to be a semiconductor with specific conductivities ranging from 10^{-6} to 10^{3} $(\Omega\ \text{cm})^{-1}$ [2]. The conductivity increases with temperature and follows the relation $\sigma = A \exp(-B/T)$ [3].

Bhide and Damle [3] investigated the properties of naturally occurring pyrolusite from various sources, some of these samples being massive and possessing crystal orientation. They studied both d.c. and a.c. conductivities and observed an anomaly in the dielectric constant of the samples at about 50 °C. This was ascribed to its ferroelectric behaviour and was discussed in relation to its crystal structure. Certain manganese minerals show a decreased conductivity in the order pyrolusite > psilomelane > manganite [4].

Wiley and Knight [5] carried out detailed conductivity studies on massive β-MnO_2 obtained by pyrolysis of Mn(II) nitrate. They reported activation energy values in the range 0.19 - 0.096 eV at −55 to 140 °C and 140 to 190 °C respectively. Room temperature resistivities varied between 20 and 70 Ω cm in the case of pressed pellets and between 0.14 and 1.0 Ω cm for *in situ* samples. This difference was attributed to strong interparticle bonding in the latter hard pyrolytic samples. They also found a change in the slope of the plot of log resistivity as a function of T^{-1} between 115 and 130 °C which is believed to be due to loss of water; it is known that the resistivity of manganese dioxide powder increases with increasing water content [6, 7].

Klose [8] reported an activation energy of 0.044 eV for pyrolytic β-MnO_2 which was ascribed to oxygen acting as a donor, but this was not proved conclusively.

Das [9] and Bhide and Dani [10] were some of the earliest to publish results on pyrolusite. From the signs of the thermal e.m.f. and the Hall constants, they concluded that manganese dioxide is an n-type semiconductor with low mobility carriers. On the other hand, MnO_2 is also reported to be a p-type semiconductor [11].

Brenet and co-workers [12 - 14] studied the effect of dopants such as Li^{+}, Th^{4+} and Cr^{3+} on the semiconductivity of pyrolytic β-MnO_2 and reported a general increase in the conductivity. Brenet [15], on the basis of an energy level diagram, also gave an explanation for the semiconductivity of β-MnO_2.

Foster *et al.* [16] studied the temperature dependency of the d.c. conductivity and the thermal e.m.f. using thermally treated samples of an electrodeposited microcrystalline γ-MnO_2. In their investigations they invoked the hopping model of Honig [17] wherein the charge carriers are electrons probably ionized from donor sites caused by oxygen deficiency. They also found an increased conductivity in an oxygen environment due to the adsorption of oxygen by the MnO_2 which enhances the electron mobility. They also pointed out that the surface layers of the MnO_2 powder

particles, whose composition may substantially differ from the bulk composition due to thermal treatment, considerably affect the results of the measurements.

Preisler [2] carried out conductivity studies which excluded surface effects with a view to investigating the role of combined water within the γ-MnO_2 crystal structure. With electrolytic manganese dioxide (EMD) and fibrous EMD obtained under different experimental conditions, Preisler observed an exponential increase in specific conductivity as the water content decreased. From the semilogarithmic relation between thermoelectric voltage and d.c. conductivity it was concluded that, for both β- and γ-MnO_2, the concentration of the conducting electrons was far below the degeneration limit. This observation was found to be consistent with the measured activation energies. It was further suggested that the water content influences the electronic band structure by successfully deforming the rutile structure of β-MnO_2 and hence the Mn–Mn distances within the lattice.

Recently Euler [18] reviewed the factors which affect the measured conductivity of compressed powders. These include the exponential influence of pressure, the anomalous exponents for several materials, the absence of any correlation with density, unexpected effects of particle size, the influence of rate of application of pressure and the laws predicting the behaviour of mixtures. McBreen [19], following the method of Glicksman and Morehouse [20], studied the variation of conductivity with pressure of a number of manganese–oxygen compounds. He plotted the resistivity as a function of the pressure and showed that the electrochemically active γ-MnO_2 has a much lower conductivity than the inactive β-MnO_2. Similar observations were made earlier by Pons and Brenet [21]. They showed that the resistivity of the manganese dioxides and the activation energy associated with semiconductivity increased in the order β- < ϵ- < γ-MnO_2. Kirchhof [22], using compressed manganese dioxide powders, showed that the pressure dependence of conductivity can be described by a simple exponential equation of the type $\sigma = Dp^{-\gamma}$, where γ is the exponent of the pressure, determined experimentally, and D is a constant. For synthetic manganese dioxides the value of γ is generally low, while for natural MnO_2 it is high. The values for EMD lie in between. This result is complemented by the earlier investigations [23, 24]. Kirchhof [22] further showed that the particle shape (as determined by scanning electron microscopy) varies with particle size and that the exponent of the pressure, which relates the specific conductivity, also included a part determined by the particle shape.

Euler and co-workers [25 - 27], reported detailed studies on the Hall effect, conductivity, thermal e.m.f. and magnetoresistance. They confirmed that both solid β-MnO_2 (natural pyrolusite) and the powder exhibit n-type conduction. The Hall mobilities reported [25] were 0.16 - 0.38 cm^2/V s (powder β-MnO_2), 0.56 and 300 cm^2/V s (solid ore samples from Caucasus and India respectively). Solid fragments of MnO_2 exhibited higher resistivi-

ities ranging from 1.9 to 15 kΩ cm. Further, according to Euler *et al.*, the carrier density varied between 2×10^{16} to 2×10^{17} cm^{-3}. They also reported that the Hall coefficient R_H of the powder increases exponentially with increasing magnetic field, $R_H \cong B^{\alpha}$. According to them, this behaviour could be best explained by assuming that β-MnO_2 behaves as a mixed semiconductor exhibiting both n-type and p-type conduction, probably by surface recombination or scattering of the carriers on the surface of powder particles. This, however, is a special case of a powder prepared from the solid samples.

The influence of mixtures of fine and coarse grained powders was also studied in relation to battery technology [28]. The effect of factors such as the matching of plates, the influence of inactive areas of the surface, of porosity and of plate thickness have all been discussed in relation to performance limits of primary and secondary batteries [29]. Euler [30] explained the *mixing rules* in connection with powder mixtures: thus, if a solid body is furnished with an ever-increasing number of randomly arranged pores, at a critical porosity, the body becomes water- or gas-permeable. A powder mixture consists of at least one less conducting species (the sponge) and one better conducting species (the pores). At a critical composition, conducting chains (clusters) are formed and the conductivity rises steeply or inversely. This explanation forms the basis of the 'percolation' theory [31, 32] and the 'effective medium' theory [32 - 34]. Euler [26] has successfully used these theories to evolve a model to explain and predict the limits of the utilization of a binary mixture consisting of a good and a bad electronic conductor, *e.g.* carbon and MnO_2 as used in a dry cell. The electronic conductivity of such a mixture and the value of its conductivity can be computed as a function of the composition of the mixture and the value of the conductivity of each powder. For MnO_2/carbon black electrodes in dry cells the limitation of the electrochemical yield can be predicted. Its quantitative value depends on the number of electric contacts per particle. Here, Euler has made an assumption that the co-ordination number is similar to the number of current carrying contacts of each of the individual particles. On this basis, he has suggested that z, that is the co-ordination number, for MnO_2/carbon black electrodes is approximately 30, and for Pb and PbO_2 is 8.

In view of the fact that carbon black forms chains in the composite mass of MnO_2/carbon black in dry cells, higher co-ordination numbers are to be found (up to $z = 32$). The critical volume of carbon black, therefore, lies below 10 vol.%. During discharge there is a change in the electronic conductivity owing to a decrease in the co-ordination number. As large amounts of $Zn(NH_3)_2Cl_2$ needles or crusts of $Zn(OH)_2$ or ZnO are formed, the co-ordination number may decrease substantially. It may, therefore, be expected that the decrease in the electronic conductivity of the active masses will be one of the factors limiting the discharge capacity.

It has been shown experimentally that the conductivity of a compact block of MnO_2 is higher than that of a thin film or loosely packed MnO_2

[35]. Electrical conductivity studies using electrolytic γ-MnO_2 [36] indicate that films of γ-MnO_2 have a low conductivity compared to powders. This is associated with different structural properties and contactability of the oxides. Several modifications of battery-grade MnO_2 were studied [37] to determine the electrical conductivity and activation energy as a function of the pH, potential and water content. There are also reports on thermal e.m.f. measurements [38] of α-, γ-, η- and δ-MnO_2 polymorphs. Albella *et al.* [39] studied the conductivity and activation energies of pyrolytic MnO_2 layers obtained by thermal decomposition of $Mn(NO_3)_2 \cdot 6H_2O$ in different atmospheres and discussed the results in relation to density, grain size and crystal structure. According to them, the energy of the donor levels produced by oxygen vacancies (n-type conduction) with respect to the bottom of the conduction band can be obtained from the slope of the log resistivity versus $1/T$ curve. The value obtained in one case was 0.015 eV. The high temperature (*i.e.* higher than the decomposition temperature) treatment of MnO_2 resulted in an increase in the activation energy and resistivity. These results, they suggested, indicate that β-MnO_2 is a compensated semiconductor with electrons and holes as carriers, the hole concentration increasing with thermal treatment. The proportion of both types of carriers in MnO_2 is probably related to the ratio of the concentrations of Mn(III) and Mn(IV) which cause the donor and acceptance levels respectively. Syed *et al.* [40] have also reported studies on the temperature dependence of the electrical conductivity of pyrolytic β-MnO_2. Euler and Helsa [41] investigated the electrical characteristics of a highly hydrated battery-grade MnO_2 powder obtained as a by-product of sachharin manufacture; the sample contained about 10 wt.% water and 7.5% KOH and was believed to be a poor crystalline form of a δ-MnO_2. Its conductivity was found to be highly dependent on pressure, with a considerable rise in transverse electric fields. They inferred that an appreciable part of the conductivity resulted from the water content, water probably forming a film between the grains. While they did not report any Hall effect measurements, it was stated to be an n-type conductor. The activation energy was reported to be 0.53 eV and found to indicate a very steep temperature dependence. Mueller [42] reported on studies of the variation of electrical conductivity of MnO_2 powder under pressure in a transverse electric field. He observed a slight increase in conductivity with increasing electric field and a more marked increase with increasing pressure. Recently, Euler [24] observed a general decrase in conductivity of a γ-MnO_2 with increasing water content. The α- and β-MnO_2 samples, however, did not follow the rule. Brenet and Faber [43] reported a new low pressure method for powder conductivity measurements. They observed that the resistivity decreased with temperature but grain size had little effect. Their activation energy values agree well with other reported values. The following sequence for the conductivity of samples was observed: (chemical, ozone) < (electrochemical) < (chemical) < (chemical, precipitated) < β-MnO_2. These results were discussed in relation to the electrochemical activity and combined water content of the samples.

They observed that the better the conductivity the worse was the electrochemical reactivity and the lower was the water content. Extending their studies to PbO_2 powders and PbO_2–MnO_2 powder mixtures they have proposed a schematic model for the conductivity mechanism in proton-containing semiconductor structures which uses $(MeO_6)_x$ octahedral structures, in every case one positive partner moving and electrons transferring or hopping into the fixed molecular structure.

2.1.1. Summary of electrical conductivity

Electrical conductivity measurements of manganese dioxides are important both from the point of view of fundamental structural investigations and electrochemical behaviour.

There seems to be a general consensus that the manganese dioxide is a mixed conductor wherein both electrons and holes participate in the conduction mechanism [25, 39]. The band structure of the dioxide, however, is not well understood and, therefore, it has not been possible to correlate the activation energy and the band gap. It would also be interesting to conduct thermal e.m.f. studies which could throw light on the nature of the second-order transition (para- to antiferromagnetic) between 76 and 84 K.

There also exist close correlations between the powder conductivity, thermal behaviour, water content and electrode potential. Hence, there is a need for further investigation in this field.

2.2. Magnetic properties

The study of the magnetic properties of various compounds of manganese has evoked considerable interest [44 - 50]. Both the methods of Faraday [51] and Gouy [52] have been used to measure the magnetic susceptibilities. Manganese dioxides are known to be paramagnetic owing to the presence of three unpaired electrons in the 3d orbitals of an Mn^{4+} ion. Amiel *et al.* [48] studied the magnetic properties of different forms of manganese dioxides (naturally occurring and artificially prepared) and found that magnetic susceptibility measurements could be used to identify the different MnO_2 polymorphs. Selwood *et al.* [49, 50, 53] identified and characterized various forms of manganese dioxides and observed the following sequence in the order of magnitude of the paramagnetic susceptibility values [53]: $\delta\text{-} > \alpha\text{-} > \gamma\text{-} > \beta\text{-}MnO_2$, the actual values lying in the range 25×10^{-6} - 45×10^{-6} at 25 °C. Recently, Parida *et al.* [54] observed the order to be $\delta\text{-} > \gamma\text{-} \geqslant \alpha\text{-} > \beta\text{-}MnO_2$. Bhatnagar *et al.* [47], from their studies on a β-MnO_2 obtained by thermal decomposition of Mn(II) nitrate, observed that reciprocal susceptibility varies almost linearly with temperature. The variation follows the Curie–Weiss law and a Néel temperature of 84 K has been observed by Bizette and Tsai [55]. Grey [56] reports on defects in magnetic susceptibility of the dioxides on the basis of an appreciable difference in atomic moments, *viz.* 2.86 μ_B observed and 3.88 μ_B derived from the spin-only relation for three unpaired electrons. He interpreted this on

the basis of Pauling's explanation of interatomic forces [57] in the first transition series wherein the interaxial 3d orbitals are involved in forming secondary cation-to-cation bonds and only 2.4 of the d electrons remain unpaired on the Mn^{4+} ion. Such secondary bonds, according to Brenet [58], would be of less significance in γ-MnO_2 than in β-MnO_2 and are compatible with the closest Mn···Mn approach, *i.e.* 2.87 Å [59]. The high susceptibility of active manganese dioxides could be due to the lengthening of Mn—O bonds [60] or a diminished paramagnetic neighbourhood [50]. The dispersed forms of MnO_2 are considered to be good examples of magnetic dilution and are expected to obey the Curie–Weiss law. In β-MnO_2, as in the case of other crystalline transition metal oxides, interactions could occur between the paramagnetic neighbours, resulting in deviation of the Weiss constants; the latter could be attributed to Heisenberg exchange effects [61], whereby $-\Delta = 2JzS(S+1)/3k$ where J is the exchange integral (variations in J are ignored); z is the co-ordination number of the equidistant paramagnetic neighbouring ions, S is the vector sum of the spin moments and is Boltzmann's constant.

On the basis of the general diagram of a rutile type of structure, *e.g.* TiO_2 [62], Brenet [63] gave an energy level diagram for a β-MnO_2. Although there is an obvious analogy between the two, in the latter case, however, an increase in the e_g levels has to be visualized to allow for the mobility of the charge carriers. According to Goodenough [64], the spontaneous atomic moment approached the spin-only value of $\mu_{Mn} = 3\mu_B$. In view of the fact that $t_{\parallel}$ one-electron and $t_{\perp}$ orbitals are half-filled according to the same model, all cation–cation, *i.e.* Mn–Mn and Mn–O_2–Mn, interactions should be antiferromagnetic as a result of the following equation:

$$4S^2J^s_{ij}\ (\text{half–half}) = -2b^2/\mu$$

This creates a competitive ferromagnetic compling between c-axis near neighbours and between corner and body-centred cations. Earlier, Yoshimori [65] had proposed a spiral screw type of structure to explain the new type of antiferromagnetic spin arrangement, wherein the spins screw along the fourfold crystalline axis. Three exchange integrals are assumed in this model, J_1, J_2 and J_3. It has been shown by Yoshimori that the first two interactions act in an antiferromagnetic way ($J_1 > 0$, $J_2 > 0$). In such a situation, three types of spin systems are possible. The stability conditions for the screw type of structure with a pitch of 7/2 seem to be realised in polianite/pyrolusite, *i.e.* $J_2/J_1 = 1.60$ and $J_3/J_1 = 0.31$. Neutron diffraction measurements [66] have confirmed the existence of a spiral spin configuration with a screw periodicity of 3.5_{cr}, the spins lying in the 001 planes. On lowering the temperature to near the Néel temperature (85 K), below which antiferromagnetism is observed, the c-axis of MnO_2 expands, leading to a distortion which can be correlated to the spin direction [67]. The spiral magnetic structure of MnO_2 [68] has been discussed by Osmond [69] in terms of superexchange interactions coupled with t_{2g}–t_{2g} interactions. Although magnetic susceptibility measurements confirm the Néel temper-

ature [55] of about 84 K, neither of these measurements, nor the neutron diffraction data, provide a reliable value for the atomic moment. The model given by Goodenough [64], based on localized $t_{\|}$ one-electrons and $b_{\pi} < b_g$, however, calls for an intra-atomic exchange splitting of the states of α-spin from those of β-spin at each cation. The stoichiometric MnO_2 is, therefore, predicted to be a semiconductor with an energy gap between the α-spin π^* and σ^* bands, similar to the gap found in $LaRbO_3$ (*i.e.* 0.2 eV). The conductivity data which are surveyed in this review, however, do not appear to be consistent with the model proposed by Goodenough in the case of β-MnO_2. The confusion is worse in the case of γ-MnO_2 as this structure is easily contaminated by H^+ ions which are electron donors to the σ^* band. A few electrons in the σ band of MnO_2 may exhibit transport anomalies at the Néel temperature.

On the basis of magnetic susceptibility measurements of the cathodic reduction products of MnO_2 at various stages of discharge, Ghosh and Brenet [70] suggested the following successive stages through which the reduction proceeds: γ-$MnO_2 \rightarrow$ lattice dilation $\rightarrow \gamma$-$Mn_2O_3 \rightarrow$ MnOOH $\rightarrow Mn_3O_4$. Similar studies were earlier reported by Selwood *et al.* [53, 71] but their interpretation, that MnO_2 reduces to Mn_2O_3, was found to be untenable [70]. The studies of Labat and Gabano [72], however, seem to support Brenet's investigations. Recently, Brenet and co-workers [73, 74] determined the magnetic susceptibilities of I.C. MnO_2 samples at various temperatures and from the values of Curie's molecular constant thus determined they could evaluate the parameters y, z, δ and m in their modified formula of the dioxides, *viz.* $(MnO_2)_y$, $(MnOOH)_z$, $\delta Mn(OH)_2$ and mH_2O. They found that the values of y correlate well with the discharge capacity of the samples determined earlier [73]. Recently, Fernandes *et al.* [75] determined the room temperature magnetic susceptibilities of chemically precipitated manganese dioxides and observed the following sequence in decreasing order of their susceptibilities: $\gamma- > (\alpha, \gamma)- > \alpha- > \beta$-$MnO_2$. Although the actual values more or less conform to the values reported by earlier workers, the order is slightly at variance with that reported by Selwood *et al.* [53]. It was also observed that, within a particular crystal phase (α or γ), Na^+-containing samples have higher values of susceptibility than those containing K^+. The linear relationship observed between the intensity I of the 100 X-ray peak and the susceptibilities was discussed in terms of the changing electron density in the *hkl* planes and the 3d orbitals. An interesting correlation was observed between I, χ and catalytic as well as electrochemical activity, suggesting a structural transition $\gamma- \rightarrow (\gamma, \alpha)- \rightarrow \alpha$-$MnO_2$. In the studies by Fernandes *et al.* [76, 77] on Fe^{3+}-doped chemical manganese dioxides, increased susceptibility was associated with increased Fe^{3+} content within a particular crystal phase, with a corresponding increase in the catalytic activity. An unusually high value for an Fe^{3+}-containing (α, γ) crystal phase could not be explained, neither on the basis of an increased Fe^{3+} impurity content nor on the basis of the above order of the χ values, and was attributed to its slightly unusual X-ray diffraction data. It is believed

that even very subtle structural variations, such as those indicated by changing intensities of particular X-ray diffraction peaks, could affect the magnetic susceptibilities of manganese dioxides.

2.3. Infrared spectroscopic studies

Parodi [78] in 1937, was one of the earliest to report the infrared spectrum of β-MnO_2, but he could not explain all the observed results. Even today the available literature on the characterization of MnO_2 polymorphs by infrared studies seems to be inconclusive. Infrared spectra of pyrolusite [79 - 81] and other manganese minerals [82 - 84] have been published by various workers. The structural changes in manganese dioxides after heat treatment at various temperatures have also been studied [85 - 87] by means of their infrared spectra, while Valetta *et al.* [88] studied the effect of various impurities. McDewitt and Baun [89], from their studies of the effect of crystallite size, reported that the characteristic band of pyrolusite only becomes apparent after fine grinding. Henning and Strobel [90] tabulated the characteristic infrared absorption frequencies of MnO, Mn_3O_4, Mn_2O_3 and MnO_2 and a collection of infrared spectra of different manganese oxides was published in 1965 [91]. More recently, Yanchuk and Povarennyk [92] presented the infrared absorption spectra and characteristic absorption frequencies of a large number of manganese oxides such as pyrolusite, ramsdellite, nsutite, birnessite, cryptomelane, hollandite and romanéchite. Infrared, spectral studies of the oxygen in manganese oxide have also been reported [93]. Faber [94] presented infrared absorption frequencies for I.C.1 (γ, electrolytic), I.C.8 (γ, chemical), I.C.11 (ρ, chlorate method), and for γ and α forms obtained by disproportionation of Mn_2O_3 in H_2SO_4. Infrared absorption curves for the I.C. MnO_2 samples have been compiled by Kozawa [95]. White and Roy [96] observed that the broad band of pyrolusite at 606 cm^{-1} splits into four ill-defined components. From a semi-theoretical analysis they found that the frequency factor (defined as $F = \bar{\nu}^2 \mu/z_1z_2$, where $\bar{\nu}$ is the main M–O stretching frequency, μ is the reduced mass of the metal–anion pair and z_1z_2 is the product of the effective charges of the cation and anion) is inversely proportional to the cube of the M–O distance. Faber [87] studied a number of infrared spectra of different types of manganese dioxides, especially those which had been chemically produced. He observed that ramsdellite shows characteristic absorptions of α and ρ forms of MnO_2: the absorption at 1100 cm^{-1} shown by α-MnO_2, however, is missing in the ramsdellite spectrum. In his study of the infrared spectra of manganese nodules recovered from French and German sources, he observed very strong absorption at 3200 cm^{-1} and 1620 cm^{-1} due to H_2O. A prominent absorption at 1080 cm^{-1} was attributed to the possible presence of Mn_3O_4.

Brenet and Faber [97] believe that the infrared frequency data, especially the shifts in the Mn–O absorption frequency, are related to catalytic and electrochemical activity. The infrared spectra can also be used to distinguish between the various crystalline phases of MnO_2 [94, 97].

Very recently, in a systematic investigation of chemically precipitated Mn(IV) oxides, Fernandes *et al.* [98] distinguished between α, γ and (α, γ) mixed crystal phases on the basis of the infrared absorption frequencies and the shape of the absorption bands. An interesting observation was the changing shape of the 700 cm^{-1} absorption band (which is quite prominent for α). It is reduced to a broad shoulder for the (α, γ) mixed crystal phase and to a slight bend or almost disappears for γ-MnO_2. Infrared spectra also help in locating the presence of OH groups, which are known to be present in active dioxides, as well as H_2O molecules, which may be present as bound water within the crystal structures [99 - 101], by virtue of their characteristic absorptions around 3400 cm^{-1} and 1620 cm^{-1}. These are attributed to the O–H stretching and bending vibrational modes respectively. The apparent absence of absorption around 1620 cm^{-1} in the α-MnO_2 samples was attributed to possibly different linkages of these OH groups in the α-MnO_2 crystal lattice with the consequent quenching of the O–H bonding vibrational mode or possible reduced degree of freedom [98]. Narita and Okabe [102] observed infrared absorption frequencies at 440 - 620, 1050, 1280, 1510, 1630 and 3400 cm^{-1} in hydrous manganese dioxides. The three additional absorption bands at 1050, 1280 and 1510 cm^{-1} were believed to be associated either with the O–H bending vibration combined with the Mn atom, or with the bending vibration of the OH group containing alkali; the latter interpretation was on the basis of the correlation between combined water and K_2O content of the samples. The intensity of these bands decreased with decreasing pH of the medium in which the samples were precipitated. Chang [103] attributed the broad absorption band at 3200 cm^{-1} in fibrous EMD to hydrogen bonding in the sample.

Recent high resolution infrared spectral measurements carried out by Potter and Rossman [104] provided information on the structure and H_2O content of various Mn(IV) oxide phases. The presence of bound water in ramsdellites was clearly observed in their spectra. Spectra of heat-treated nsutites indicated possible concentrations of randomly distributed pyrolusite domains with rising temperature. These studies also showed that:

(a) birnessite has a layer structure,

(b) synthetic buserites and birnessites have analogous layer structures,

(c) the shift from the 10 Å to 7 Å spacing in the X-ray diffraction is caused by water loss rather than by a structural rearrangement of the [MnO_6] framework, and

(d) natural todorokite is a valid mineral (not a mixture of buserite and its decomposition products birnessite and manganite).

2.4. Thermoanalytical investigations

Manganese dioxides have been extensively studied by thermoanalytical methods, including thermogravimetry (TG), differential thermogravimetry (DTG) and differential thermal analysis (DTA). On heating, the dioxides follow the reaction sequence [105]

$$MnO_2 \xrightarrow{I} Mn_2O_3 \xrightarrow{II} Mn_3O_4 \xrightarrow{III} MnO$$

and it is generally agreed that the transformation temperatures in air for reactions I and II are around 550 °C and 950 °C, respectively [106, 107]. There are, however, conflicting interpretations of the endothermic peak in DTA between 1160 and 1230 °C. Dollimore [108, 109] attributed it to reaction III, but it has been shown to be reversible on cooling [110, 111] and is believed, by some, to be due to a polymorphic transformation of tetragonal Mn_3O_4 to a cubic γ form [112]. The latter interpretation was apparently confirmed by Tinsley and Sharp [105], whose X-ray analyses of samples heated to 1300 °C showed the presence of Mn_3O_4 only. On the other hand, samples heated to 1500 °C in nitrogen and cooled in nitrogen showed the presence of MnO only. An exothermic peak for reaction III is to be expected, therefore, between 1500 and 1600 °C in nitrogen [105].

The effect gaseous environments, such as air, oxygen, nitrogen and argon, have on the decomposition temperatures, especially for the reaction $MnO_2 \rightarrow Mn_2O_3$, has been studied by various workers [113 - 116]. It is generally observed that the decomposition temperature is higher in oxygen and lower in inert gases. The shift to higher temperatures and the increase in sharpness of some decompositions when carried out in an atmosphere of the evolved gas was already known. Garn [117] explained it on the basis of complete, or at least partial, reversibility of the decomposition process and consequent application of the law of mass action. Reversibility is considered by some workers to be the reason for the unsuitability of an oxygen environment for investigations of partially reduced manganese dioxides [118, 119]. Low peak decomposition temperature has also been ascribed to the fineness of the MnO_2 particles [120]. Manganese dioxides, however, are usually sufficiently porous [121 - 124] for the surface to be independent of the particle size, which should not, therefore, have an effect on the decomposition temperature, as was observed by Freeman *et al.* [116]. The latter also observed that the temperature was not affected by changes in the rate of gas flow in the range 1 - 4 litres per hour. Thermal investigations under reduced pressures (50 mmHg), however, lowered the decomposition temperatures to about 430 and 840 °C for reaction I and II, respectively. Thermodynamic considerations [125] indicate that the various decomposition temperatures depend on the partial pressure of oxygen, whereas the temperature of the polymorphic transformation will not be affected. Brenet *et al.* [126] studied the kinetics of thermal decomposition of α-, β- and γ-manganese dioxides and determined the corresponding activation energies. From a study of the oxygen pressures generated in reactions I and II, Matsushima and Thoburn [127] evaluated the enthalpy changes of these reactions. Kozawa [128] calculated the enthalpies of formation of manganese dioxides from the changes in their decomposition temperatures. Koshiba and Nishizawa [129] calculated the desorption enthalpies in the range 54 - 180 kJ (mol H_2O)$^{-1}$ from the differential thermograms. Recently

Sato *et al.* [130] observed that a disordered EMD decomposes at a lower temperature than a better crystallized EMD.

TG and DTA are dynamic techniques and the thermograms obtained, therefore, depend upon the precise conditions and the environment employed [131, 132]. It follows that little is to be gained by comparison with previously published thermograms [116]. The first systematic thermal study in conjunction with X-ray analysis was reported by McMurdie and Golovato [133] who identified various crystalline phases of MnO_2. Thermal analysis has also been employed for the characterization of manganese oxide minerals [134 - 136] and for identifying mineral phases where X-ray and optical methods fail [137]. It has been observed that pure ramsdellite changes to pyrolusite at 500 °C and that psilomelane-like minerals exhibit a broad exothermic effect in the range 800 - 1000 °C [134]. Various types of natural and synthetic Mn(IV) oxides have been characterized by DTA and the activation energies for the decomposition processes have been reported [138, 139]. Investigations of manganese dioxides by simultaneous TG/DTG and DTA have been found to be very informative [140]. Manganese dioxides obtained by the thermal decomposition of $MnCO_3$ [141] and $Mn(NO_3)_2$, when thermally investigated under various environments [142 - 146] such as nitrogen, oxygen, continuous vacuum, nitrous oxide or water vapour, are known to produce reduced oxides of varying composition. δ-MnO_2 obtained by reduction of sodium or potassium, permanganates with $MnCl_2$ [147] showed a broad endotherm between 20 to 250 °C due to water loss, followed by an exothermal structural rearrangement process, although they retained the same X-ray pattern. Decomposition temperatures around 500 and 900 °C were obtained for reactions I and II respectively. The thermal behaviour with respect to the decomposition temperature of an electrolytic MnO_2 has also been discussed in relation to the way in which it was prepared [148].

TG and DTA studies of hydrous manganese dioxides, including synthetic β- and γ-MnO_2, have been reported [102] which indicated that their thermal characteristics are influenced by the K:Mn molar ratios. The thermal behaviour of Mn(IV) oxides should, therefore, be interpreted in relation to their K^+ content. The hydrous MnO_2 samples (K:Mn molar ratio 0.1 - 0.3) showed an exothermic peak at 450 °C which was believed to be due to the transformation to α-MnO_2. This peak became larger and sharper at the molar ratio of 0.125. The thermogram of some of these samples showed a loss of combined water up to about 900 °C which is confirmed by infrared spectroscopy.

Brenet and Grund [149] could distinguish between inactive pyrolusite, chemical and electrolytic manganese dioxides by thermogravimetry. They related the differences in catalytic and electrochemical activity to the differences in decomposition temperature and, thus, to the differences in their crystal structures [150]. Fishburn and Dill [145] reported that the decomposition temperature of MnO_2 to Mn_2O_3 increased in the following order: electrolytic MnO_2 and activated ores < battery active $\rho(\gamma)$ ores <

pyrolusite β-ores. Lee and his collaborators [116, 151] studied the thermal decomposition of both natural and synthetic manganese dioxides and related the peak decomposition temperature of the MnO_2 to Mn_2O_3 transformation to their electrochemical activity. According to their studies, a low peak decomposition temperature indicates high battery activity. They also observed a good correlation between peak decompositon temperature and crystalline type, thus confirming the findings of Fishburn and Dill [145] and refuting the suggestions of Glemser *et al.* [152] that thermogravimetric analysis cannot differentiate MnO_2 modifications. Recent studies of Fernandes *et al.* [75] indicated that chemically precipitated α-MnO_2 samples decompose to Mn_2O_3 at slightly lower temperatures than the corresponding γ-MnO_2 samples, although the former have much less electrochemical activity.

The above conclusions of Freeman *et al.* [116] appear, therefore, to be valid within a particular crystal phase type. Fernandes *et al.* [75] also observed that within α or γ crystal phases, low peak decomposition temperature is associated with high electrochemical activity. It may be mentioned here that there are earlier reports [153] of cryptomelanes decomposing at a higher temperature than pyrolusite to form either α- or γ-Mn_2O_3.

A flattish split endotherm in the DTA (temperature range 500 - 570 °C) observed by Varma [154] for $MnO_2 \rightarrow Mn_2O_3$ transformation in an electrolytic MnO_2 containing co-deposited Fe is attributed to the simultaneous occurrence of endo- and exothermic processes of the type observed by Paulik *et al.* [155]. The endothermic process is believed to be associated with rupture of valence forces between the MnO_2 complex and Fe. The exothermic process could be due to formation of an iron oxide with its subsequent dissolution in Mn_2O_3 to form a solid solution resulting in a new compound of high heat resistance. The latter fact is apparently confirmed by the fact that it decomposes to Mn_3O_4 at a higher temperature than in the case of Mn_2O_3 obtained from electrolytic MnO_2 containing Fe. Brenet suggests the determination of the percentage of ionic and covalent bonds between cations and oxygen to explain the observed results. Recently, a similar effect has been observed by Fernandes [77] in chemically precipitated Mn(IV) oxides belonging to α and γ crystallographic forms with Na^+, K^+ and Fe^{3+} incorporated in their lattice. While no explanation was attempted for the origin of this type of endothermic peak, it appeared that only relatively large amounts of Fe^{3+} in the γ-MnO_2 lattice, and the presence of Na^+ ions in the α-MnO_2 lattice, are responsible for the observed effect.

Thermal investigation of the water content in manganese dioxides has received tremendous attention over the years. Water content is probably the one factor which is directly or indirectly responsible for the complexities of chemical/electrochemical reactivity and thermodynamic stability of the various MnO_2 phases. Water, in the form of neutral molecules or hydroxyl groups, seems to be responsible for the crystal lattice variations and consequent changes in electrical conductivity, electrode potential, etc. Recently, Preisler observed a linear relation between the electrode potential and the

combined water with a break during the $\gamma \rightarrow \beta$ transition [156]. As early as 1928, Jegge [157], and later Sasaki and Kozawa [158], emphasized the importance of H_2O in active dioxides. A decrease in the discharge capacity was observed by Sasaki and Kozawa [159], Fukuda [160] and Drotschmann [161] as the water content fell. Droschmann [162] claimed that the electron acceptability depended on the degree of hydration in addition to lattice distortion. Water is also known to help proton migration in the lattice [150, 163]; Glemser *et al.* confirmed the presence of OH groups in manganese dioxides by DTA measurements [152, 164], infrared [165] and magnetic resonance spectroscopy [152, 166] and the absence of OH groups in ramsdellite and in β-MnO_2 [164], thus supporting the observation of Brenet and co-workers [126]. Tvarusko [167] determined the water content of various types of manganese dioxide (natural, electrolytic, chemical and hydrous) equilibrated in an atmosphere of 75% relative humidity by heating them to temperatures of 110, 235 and 400 °C. The total water content varied from 1%, for a highly crystalline β-MnO_2, to 20% in the case of almost amorphous, synthetic hydrous MnO_2. Electrolytic MnO_2 has a lower total water content than chemical MnO_2, but this is reversed for the constitutional water which is released between 110 and 400 °C [167]. Water released below 110 °C is that which is physically adsorbed. The dependence of the water content of MnO_2 on its type, origin and preparative conditions is well established [167 - 170]. The water lost at 110 °C decreases according to the series: natural ore < electrolytic < chemical < synthetic hydrous manganese dioxide [170]. Studies of Amlie and Tvarusko [171] indicated that the combined water is surface dependent. The studies of Tye [172], however, lead one to believe that the OH groups are uniformly distributed throughout the bulk of the solid. In γ-MnO_2, Mn^{3+} and OH^- ions exist in dissociated form, while in other varieties MnOOH remains in an undissociated state.

Lee *et al.* [173, 174], by a systematic temperature programmed desorption (TPD) technique, identified three types of water:

(I) Physisorbed molecular water was released at around 100 °C and was probably due to water firmly hydrogen-bonded to the underlying surface hydroxyls.

(II) A second type was associated with the irreversible loss of water between 160 and 250 °C and which could be partially resolved into two components [174]. The first component (IIa) appeared to have been originally held in the bulk of the oxide while the amount of the second component (IIb) was directly related to the overall oxidation state of the oxide and was attributed to the removal of water by condensation of hydroxyls.

(III) This type appeared between 320 and 360 °C and was poorly resolved in near vacuum, nitrogen or water vapour environments. It was clearly resolved only in oxygen.

Activation energies of desorption were evaluated for types I, II and III and a model consistent with these obervations was proposed. A better insight was provided by thermal investigations of γ-MnO_2, and some reduced forms,

in oxygen [175, 176]. These samples were represented by the general formulae $(1-x)MnO_2 \cdot xMnOOH$ where $x = 1$ signifies groutite α-MnOOH.

The TG/DTG studies of Lee *et al.* [176] in an oxygen environment with samples in the compositional range $0.11 \leqslant x \leqslant 0.35$ indicated an increased type I water with x. It was ascribed to the presence of additional hydrogen-bonded water adsorption, following the increase in surface hydroxylation which accompanies chemical reduction. There was a general decrease for type II from $x = 0.11$ to $x = 0.14$. Type IIb, which featured more clearly in the range $x = 0.18 - 0.35$, was believed to follow a Brouillet mechanism [119] involving endothermic dehydroxylation of the oxyhydroxide component of $(1-x)MnO_2 \cdot xMnOOH$ with simultaneous exothermic oxidation in accordance with the overall reaction

$$4MnOOH + O_2 \longrightarrow 4MnO_2 + 2H_2O$$

The dependence of type II water on x at values $x > 0.5$ was thought to follow a different mechanism involving the formation of an intermediate corundum phase which was less susceptible to oxidation and formed in accordance with the following reactions:

$$2MnOOH \longrightarrow Mn_2O_3(\text{corundum}) + H_2O$$

$$2Mn_2O_3 + O_2 \longrightarrow 4MnO_2$$

The latter reaction explains the accompanying absorption process observed in the DTG curves. X-ray diffractive traces at $x > 0.5$ (which suggest a solid solution limit) indicated the formation of an oxyhydroxide which did not exactly conform to the groutite structure. The anomalously high magnetic moments at $x > 0.5$ were attributed to orbital contributions following structural reorganization and consequent distortion of octahedral symmetry. The latter was probably an implication of Jahn–Teller distortion leading one to think that there was a solid solution in the range $x = 0 - 0.5$.

At high oxygen pressures, type III was found to be resolved into two components in the temperature range 300 - 400 °C. Type IIIa was ascribed to a $\gamma \rightarrow MnO_2$ phase transition, probably accompanied by a crystallographic shear defect in the newly formed pyrolusite lattice. The IIIb water could be a consequence of the reaction:

$$Mn(OH)_4 \xrightarrow{O_2} MnO_2 + 2H_2O$$

The observed decrease in type III water with increasing levels of initial chemical reduction may mirror the reductions [176]

$$Mn(OH)_4 + H^+ + e^- \longrightarrow MnOOH + 2H_2O$$

$$Mn(OH)_4 + 2H^+ + 2e^- \longrightarrow Mn(OH)_2 + 2H_2O$$

The formation of Mn_5O_8 from groutite reported by earlier workers [177] could not be observed, but a subsequent investigation by the same

group [178] in an argon atmosphere confirmed the presence of Mn_5O_8, which could have been formed by the reaction

$$(1-x)MnO_2 \cdot xMnOOH \longrightarrow \frac{x}{4}Mn_5O_8 + \frac{n}{2}H_2O + \frac{4-5x}{4}MnO_2$$

Miyazaki [179], in his mass spectrometric studies of water released from samples heated under vacuum, observed the evolution of three main gases, H_2O, O_2 and CO_2, with water release occurring predominantly at temperatures 100, 200 and 300 °C, analogous to types I, II and III, respectively, as reported by Lee *et al.* [173]. Types I and II, II and III, and III were found to be the predominant types of waters in chemical, electrolytic and natural MnO_2 samples, respectively. The type present was governed by the kinetics of formation of the particular type of MnO_2, *e.g.* the high reaction rate of formation of chemical MnO_2 reduced types II and III in the crystal lattice compared to the other samples. Superiority in discharge performance is attributed to the combined effect of water types II and III *vis-à-vis* the relative oxygen mobility in the MnO_2 lattice. The high oxygen pressure and greater percentage of types II and III are believed to be responsible for the superiority of the electrolytic manganese dioxides.

The thermogravimetric method cannot usually be used for measurements of water loss as it is indistinguishable from oxygen evolution, especially at higher temperatures. Although this drawback was overcome by mass spectrometric measurements [173, 174, 179] the data were not so precise and the heating rates were usually too high for equilibrium to be reached. Yoshimori *et al.* [180] recently evaluated the water contents of some I.C. MnO_2 samples by a coulometric method which was believed to ensure a more precise and accurate determination of micro-amounts of water, without the use of reference materials [181 - 183]. The data obtained were discussed in relation to Erday's classification of water contents [184]. They concluded that the water is of two types:

(i) loosely bound water removed around 100 °C, and believed to be present in the fine pores;

(ii) strongly bound water, thought to be possibly due to dehydroxylation of OH groups adhering to the pore walls.

3. Electrochemical properties

3.1. Cathodic reduction mechanism

Manganese dioxides are used extensively as active cathode materials in Leclanché or alkaline Zn/MnO_2 cells. Electrochemically the cells may be represented as:

$$\begin{array}{c|c|c} (-) & & (+) \\ Zn(s) & \text{Electrolyte} & MnO_2, C \end{array}$$

The nature of the cell reaction depends on the nature of the electrolyte and also on the discharge conditions [185]. Thus, for a Leclanché cell,

$$2MnO_2 + 2NH_4Cl + Zn \longrightarrow 2MnOOH + Zn(NH_3)_2Cl_2 \quad (1)$$

for a zinc chloride cell,

$$8MnO_2 + 8H_2O + 4Zn + ZnCl_2 \longrightarrow 8MnOOH + ZnCl_2 \cdot 4Zn(OH)_2 \quad (2)$$

and for an alkaline cell,

$$2MnO_2 + H_2O + Zn \longrightarrow 2MnOOH + ZnO \quad (3)$$

It is thus seen that MnOOH is the major cathode reduction product in all Zn/MnO_2 cells and represents the end of one-electron exchange. This is confirmed by X-ray diffraction studies [186 - 188], which indicate that the oxyhydroxide has a crystal structure similar to that of the mineral, groutite (α-MnOOH). Brenet and co-workers [189 - 190] showed that, on the initial reduction of γ-MnO_2, the basic crystallographic structure does not change but only expands as OH (r = 1.53 Å) and Mn^{3+} (r = 0.62 Å) take the place of O^{2-} (r = 1.4 Å) and Mn^{4+} (r = 0.52 Å) ions. Progressive dilation of the structure of γ-MnO_2 with reduction is confirmed for cathodic reduction in NH_4Cl [188, 191], in $NH_4Cl/ZnCl_2$ [186], in alkaline electrolytes [187, 192 - 194], and during chemical reduction [195 - 197]. Potential measurements have also confirmed that the reduction takes place in a homogeneous phase [172, 198 - 200].

Kozawa and Powers [201] suggested that the cathodic reduction takes place by the incorporation of protons and electrons into the MnO_2 lattice:

$$MnO_2 + H_2O + e^- \longrightarrow MnOOH + OH^- \quad (4)$$

The protons originate from the water molecules adsorbed from the solution onto the surface of the manganese dioxide and not from the OH groups of the combined water. The above mechanism hints at a mobile equilibrium with the positions of Mn^{4+} and Mn^{3+} ions constantly changing by electron exchange and the protons constantly attaching themselves to different oxygens.

From eqn. (4) it can be shown that the changes in electrode potential are governed by the factor

$$RT \ln(a_{MnO_2}/a_{MnOOH})$$

where R is the gas constant, T the absolute temperature and a the activity of the compounds involved.

As the reduction takes place in a homogeneous phase, the activity terms progressively decrease during discharge. This is the reason for the characteristic sloping of the discharge curves of MnO_2 cathodes [185] (see Fig. 1). If the products were to exist as separate phases, then their activities would have remained unchanged and thus a constant potential would have been observed throughout the discharge (Fig. 1(b)).

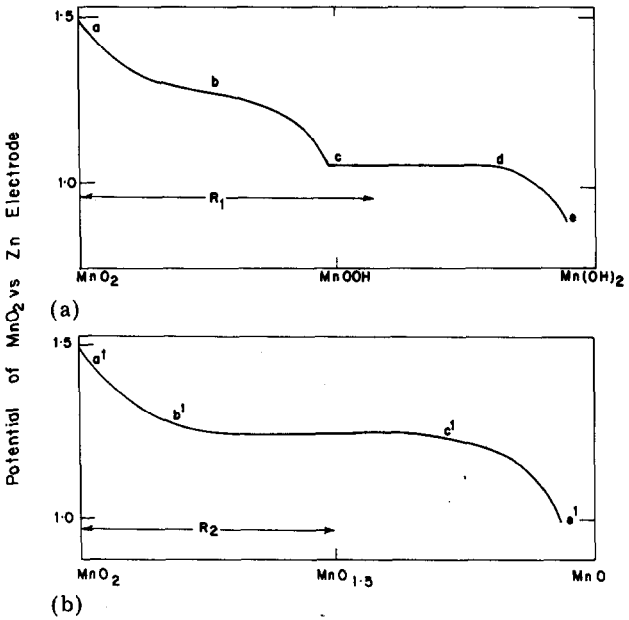

Fig. 1. Schematic semi-ideal discharge curves of MnO_2 in (a) 9 M KOH and (b) 5 M NH_4Cl + 2 M $ZnCl_2$ solutions. R_1 = range of discharge capacity of a commercial alkaline MnO_2/Zn cell; R_2 = range of discharge capacity of a commercial Leclanché or zinc chloride cells.

Kozawa [202] explained that in the curve of Fig. 1(a) (obtained in alkaline electrolyte), region a to b, in the first step, corresponds to homogeneous reduction with no change in the lattice structure. The region b to c corresponds to homogeneous reduction with possible slight deterioration in the lattice structure, while the region c to d (second step) corresponds to heterogeneous phase reduction:

$$MnOOH + H_2O + e^- \longrightarrow Mn(OH)_2 + OH^- \quad (5)$$

This takes place by a dissolution–precipitation mechanism [203], as follows:

$$MnOOH \longrightarrow [Mn(OH)_4]^- + e^- \longrightarrow [Mn(OH)_4]^{2-} \longrightarrow Mn(OH)_2$$

initial solid-phase ↓ dissolution process

electrochemical reduction at graphite surface

↓ precipitation process final solid-phase

The solubility of Mn(II) and Mn(III) ions was found to increase rapidly with increasing KOH concentration owing to the formation of complex ions with OH^-, *e.g.* $[Mn(OH)_4]^{2-}$ [204]. This explains the increasing depth of discharge of the heterogeneous phase reduction step with the increase in KOH concentration. A similar effect is also observed in the presence of a complexing agent such as triethanolamine (TEA). KOH concentration,

carbon content of the cathode mix and MnO_2 particle size were found to have no effect on the homogeneous phase reduction step [205]. Since the second step proceeds through dissolved Mn(III) ions followed by reduction on the graphite (carbon) surface, its discharge depth increases when the quantity of graphite in the cathode mix is increased. The particle size of MnO_2 also has a similar effect on the second step [205 - 207].

In the $NH_4Cl/ZnCl_2$ electrolyte, the portion a′ to b′ of Fig. 1(b) corresponds to homogeneous reduction (eqn. (4)). The only difference from the curve in Fig. 1(a) is the concentration polarization due to the pH change of the electrolyte. Since OH^- ions are released, the pH of the solution tends to increase. The second step, b′ to c′, in addition to eqn. (4) is due to the heterogeneous phase reaction

$$MnO_2 + 4H^+ + 2e^- \longrightarrow 2H_2O + Mn^{2+} \quad (6)$$

Equation (4) for the homogeneous phase reduction limits the useful discharge capacity of practical cells (a to c of Fig. 1(a) and a′ to b′ of Fig. 1(b)) [202].

Whether or not the end-product MnOOH of the first step is equivalent to $MnO_{1.5}$ or to $MnO_{1.6}$ is controversial. In alkaline solution Kozawa and Powers [201, 208] suggest $MnO_{1.5}$, while others [193, 209] report the end-member to be $MnO_{1.6}$. The latter could perhaps be stable in an alkaline electrolyte by the incorporation of K^+ ions from KOH [209]. The compound Mn_5O_8, equivalent to $MnO_{1.6}$, has been synthesized [210 - 211].

There are also conflicting reports about the states of reduction between $MnO_{1.75}$ and $MnO_{1.5}$ [212]. Extra lines appear in the X-ray diffraction pattern which are difficult to assign owing to the diffuse nature of the spectrum. The compounds proposed include γ-Mn_2O_3 [189], manganite, *i.e.* γ-MnOOH [189, 213, 214], and groutite, *i.e.* α-MnOOH [195, 199]. Gabano and co-workers [195] suggested that the structure reorganizes at $MnO_{1.75}$ from γ-MnO_2 to ramsdellite–groutite. The tendency for the diffraction pattern to become diffuse at this mid-point under certain conditions [186, 215] supports this argument. Maskell and co-workers [212, 216], in an extensive investigation using X-ray diffraction techniques on chemical and electrochemical reduction of γ-MnO_2, drew the following conclusions:

(1) The chemical or electrochemical reduction of —MnO_2 proceeds via a single phase over the complete range MnO_2 - $MnO_{1.5}$.

(2) The end-member, $MnO_{1.5}$, has been named —MnOOH to distinguish it clearly from groutite.

(3) Accepting the de Wolff model [217] for —MnO_2 then —MnOOH is an intergrowth structure of groutite with microdomains of manganite.

(4) Between $MnO_{1.75}$ and $MnO_{1.9}$ oxyhydroxide is metastable and —MnOOH slowly precipitates as a separate phase in aqueous solution, probably by a dissolution–precipitation mechanism.

(5) In the range MnO_2 - $MnO_{1.75}$ an electron entering the structure is delocalized between two adjacent Mn^{4+} ions.

(6) In the region $MnO_{1.75}$ - $MnO_{1.5}$ an added electron displaces a shared electron and the two electrons are associated with individual cations forming Mn^{3+} ions.

Not all of the polymorphs of manganese dioxide undergo homogeneous phase reduction in the range MnO_2 - $MnO_{1.5}$. Bode *et al.* [197] and, very recently, Fernandes *et al.* [218] reported a very narrow range of compositions (MnO_2 - $MnO_{1.96}$) for the homogeneous reduction of β-MnO_2. Bell and Huber [209] suggested that homogeneous reduction is also possible in the range $MnO_{1.8}$ - $MnO_{1.6}$. Using β-MnO_2 obtained by the heat treatment of electrolytic γ-MnO_2, Kozawa and Powers [208] found that a homogeneous reduction occurs over the entire range MnO_2 - $MnO_{1.5}$. The results of Fernandes *et al.* [208] indicated that, for α-MnO_2, the single-phase reduction occurs up to around $MnO_{1.82}$, and that this range of composition increases with the increase in γ-MnO_2 domains within the α form. The discharge curves for α, β and γ forms of manganese dioxides obtained from various sources have been recently reported by Kanungo and co-workers [219].

The role of the new concept "one-phase solid redox system" typified by MnO_2 in physical chemistry and electrochemistry has been repeatedly emphasized by Kozawa [220]. This is especially valid in the light of the reports of some other compounds, such as $RuO_2 \cdot xH_2O$ [221], MoO_3 [222], TiS_2 [223], and possibly other sulphides and oxides [224] which behave similarly. The concept is useful to explain the catalytic and electrochemical properties of these oxides which, otherwise, could not be satisfactorily explained.

3.2. Calculated and observed potentials

Considerable attention has been given to predicting the electrode potentials of the system MnO_2–MnOOH [201, 208, 225]. Calculations of Neumann and v. Roda [226] indicated widely differing activity coefficients for MnO_2 and MnOOH at various stages of discharge. Kozawa and Powers [201, 208] replaced the activity terms in the expression

$$E = E^0 + \frac{RT}{F} \ln \frac{a_{MnO_2}}{a_{MnOOH}} \tag{7}$$

by mole fractions X_{MnO_2} and X_{MnOOH} which can be calculated from the stoichiometry of the solid solution. The curves thus obtained, however, showed insufficient rate of fall of potential when compared with the observed values [208, 227, 228]. Tye [172] obtained a better representation by using ion mole fractions:

$$RT \ln \frac{X_{Mn^{4+}} X_{O^{2-}}}{4 X_{Mn^{3+}} X_{OH^-}}$$

where

$$a_{MnO_2} = \frac{27}{4} X_{Mn^{4+}} X_{O^{2-}} \tag{7a}$$

and

$$a_{MnOOH} = 27 X_{Mn^{3+}} X_{O^{2-}} X_{OH^-} \tag{7b}$$

on the assumption that the solid-phase redox system represents an ideal ionic solution. Interestingly, the converse is found to be true for β-MnO_2. Tye also argued that the MnOOH is undissociated in β-MnO_2 and fully dissociated in a γ-MnO_2, *i.e.* the constituents of MnOOH have no independent existence. Assuming $(MnOOH)_r$ equivalent to a mixed oxide $(MnO_2)_{1-r}(MnOOH)_r$, Atlung and Jacobsen [229] obtained the relation

$$E = E^\theta + \frac{RT}{F} \ln \frac{1-r}{r}$$

for the reduction

$$MnOOH_r + \delta H^+ + \delta e^- \longrightarrow MnOOH_{r+\delta}$$

where $0 < r < 1$ and $\delta \to 0$; r is considered as an independent variable. Plots of the open-circuit voltage $E - E_{r=0.5}$ as a function of r, however, showed large deviations from the observed curves. Atlung and Jacobsen therefore attempted to explain the discharge mechanisms using a novel approach. They considered MnO_2 to be an "insertion electrode" analogous to the intercalation electrode, *e.g.* Li/TiS_2, in which the inserted protons and electrons are not assigned to discrete chemical compounds like MnOOH. Instead, their statistical distribution on the available sites (for protons) or bands (for electrons) in the lattice was the basis for deriving an analytical expression for the potential:

$$E = E^\theta + \frac{RT}{F} \ln \frac{1-r}{r} - \frac{\mu e}{F} \tag{8}$$

where μ_e is the electrochemical potential for the insertion of an electron in the MnO_2 lattice. In eqn. (8), E is sensitive to the influence of the electronic term and from this the following was derived:

$$E = E^\theta + \frac{2RT}{F} \ln \frac{1-r}{r} \tag{9}$$

This gave good agreement for $r < 0.5$, but not for $r > 0.5$.

Subsequently, Maskell *et al.* [230] independently showed that, by introducing a spatial correlation coefficient,

$$\bar{E} = E^0 + \psi \frac{RT}{F} \ln \frac{1-r}{r} \tag{10}$$

the observed potential $\bar{E}$, corrected for pH, agreed well with the observed values.

In deriving this expression Maskell *et al.* considered Mn^{4+}, Mn^{3+}, O^{2-} and OH^- to be thermodynamically independent with the protons and electrons having independence of position and motion in their movements across the lattice of the dioxide. According to them, when there is no spatial correlation of the protons and electrons, ψ takes the value of 2 and, therefore, eqn. (10) reduces to

$$\bar{E} = E^0 + \frac{2RT}{F} \ln \frac{1-r}{r} \tag{11}$$

This is identical with eqn. (9) which was for an alkaline medium, whereas eqn. (11) was for a neutral or acid electrolyte.

Atlung and Jacobsen [229], however, derived a slightly modified expression which fits the experimental data rather well:

$$E = E^\theta + \frac{2RT}{F} \ln \frac{0.8-r}{r} \tag{12}$$

although eqn. (13), given below, completely reproduces the measured potentials:

$$E = E^\theta + \frac{2RT}{F} \ln \frac{[1-(1+r)r]^{1+\alpha}}{r(1+\alpha r)^\alpha} \tag{13}$$

where α is a term introduced to account for the number of sites not available for proton insertion. The value of α is obtained from the relation

$$r_{max} = \frac{1}{1-\alpha}$$

where r_{max} is the value at the end of homogeneous reduction and is obtained from the observed discharge curve. Subsequently, however, Fernandes *et al.* [218] observed discharge curves which indicated that Atlung and Jacobsen's result is not universally applicable. A slight change in the structure, such as an increase in the number of defects, can change the electronic term in particular. The number of allowed sites can also vary, for example with the amount of intergrown β or δ domains [231].

Earlier, Tye [172] was able to account quantitatively for potentials at low degrees of γ-MnO_2 reduction. The underlying assumption was that Mn(III) in the parent γ-MnO_2 was inactive towards the potential-determining reaction. Subsequently, Maskell *et al.* [232] provided thermodynamic evidence indicating that the inactive Mn(III) may be equivalent to $r = 0.06$ - 0.08 in $MnOOH_r$ [230, 232]. According to them, it may be either due to small amounts of a separate phase such as Mn_2O_3 or to some structural disorder resulting in certain Mn atoms being in a co-ordination unfavourable to the quadrivalent state. Following up this work with a statistical thermodynamic approach to the oxyhydroxide potentials of the system γ-MnO_2–δ-MnOOH, Maskell and co-workers [233, 234] obtained a good correlation between the observed and the theoretical potentials.

Preisler [235] attempted to explain the lowering of the electrode potential of EMD upon heat treatment from a thermodynamic approach, wherein the electrode potential was based on the galvanic cell:

$$Pt|H_2(p_{H_2} = 1)|H^+(aq)||H^+(aq)|MnOOH|MnO_2|Pt$$

For the overall cell reaction, $MnO_2 + \frac{1}{2}H_2 = MnOOH$, for which the Nernst equation in the Vosburgh form is

$$E = E^0 + 0.059 \log \frac{a_{Mn^{4+}}}{a_{Mn^{3+}}} + 0.059\ pH$$

where

$$E^0 = -\Delta G/F$$

Preisler explained the potential changes of heat-treated EMD by making use of the above equation in differential form:

$$\frac{dE^0}{dm} = -\frac{1}{F}\frac{m\ d(\Delta G)}{dm}$$

where m is the mole concentration of combined water in MnO_2. This highlights the importance of combined water in the electrode potential studies.

Tye [185] also found that the observed open-circuit potentials of the Zn/MnO_2 cells deviated (by less than 120 mV) from the calculated values based on the Gibbs free energies of the reactants and products. This was not surprising as it is not possible for the reactants and products of a homogeneous-phase redox system to have a unit activity coefficient. Evaluation of the activity terms of the MnO_2–MnOOH system using eqns. (7a) and (7b) gave good agreement between the observed and the calculated values. It should be noted that no deviations were observed for cell systems such as Ag_2O/Zn where the reactants and products remain as heterogeneous phases through the discharge process.

3.3. Potential–pH relations

Although water is consumed in alkaline Zn/MnO_2 cells during discharge, the pH of the electrolyte remains unchanged. The pH does change, however, during the discharge of Leclanché types of cell, in accordance with the potential-determining relation

$$MnO_2 + H_2O + e^- \longrightarrow MnOOH + OH^-$$

By the Nernst equation, it follows that, at 25 °C,

$$E = E' - 0.0592 \log \frac{[Mn^{3+}]}{[Mn^{4+}]} - 0.0592\ pH$$

This implies that the potential of MnO_2 should decrease by 59.2 mV per unit increase in pH. Slopes of E *vs.* pH curves numerically greater than 59.2 mV pH^{-1} observed by various workers [236 - 240] could be attributed

to ion-exchange properties of MnO_2 [241 - 243]. This was confirmed by Benson *et al.* [244] and could explain the change in slope.

According to Kozawa [242], water molecules physisorbed on the manganese dioxide surface are the sites for ion exchange.

The equation implies a steady rise in pH with increasing ion exchange and with the associated increase of OH^- concentration at the MnO_2 surface [243, 244]. That the pH response is governed by the surface characteristics was also confirmed by Kozawa's studies [245] of heat-treated manganese dioxide having a surface layer of lower oxide.

Recently, Caudle *et al.* [246, 247] showed that acid-treated β-MnO_2 had a potential response very close to the theoretical value of 59 mV pH^{-1} in the absence of Mn^{2+} ions, ostensibly removed by acid treatment. The same slope was also obtained for dioxides in the absence of all cations except H^+, when cation exchange is not possible. Further, in the presence of Mn^{2+}, the pH response was again about 112 mV pH^{-1}, close to the theoretical value. Kozawa [248] obtained a 120 mV pH^{-1} slope for potential studies in dilute NH_4Cl or HCl solution at low pH, while a 60 mV pH^{-1} slope was obtained for $ZnCl_2$ solution even at low pH (0 - 5). Unfortunately, no explanation was found for the discrepancy.

Very recently, Tari and Hirai [249 - 251] showed that two different slopes are obtained in the case of synthetic β-MnO_2 in the pH ranges 3 - 7 and 7 - 9. Attempts to remove Mn^{3+} ions (which, by disproportionation, give rise to Mn^{2+} ions in the electrolyte, thus causing a steeper slope) by acid treatment were unsuccessful. In the presence of $ZnCl_2$ and $(C_2H_5)_4NClO_4$, however, the pH response was 60 mV pH^{-1} in the pH range 4 - 7. If NH_4Cl–HCl was used, the pH response changed from 75 to 100 mV pH^{-1} in the pH range 1 - 2.5, which is due to the disproportionation reaction of Mn^{3+}. Their conclusion was that the presence of supporting electrolytes such as $ZnCl_2$ and $(C_2H_5)_4NClO_4$ inhibits the disproportionation reaction and thus a slope close to the theoretical value was obtained. In their studies of I.C. MnO_2 samples (γ and β) in NH_4Cl solution [252] they observed that:

(a) each *E vs.* pH relation was composed of two straight lines of different slopes, and

(b) the equilibrium acid base point coincided fairly well with the pH value at which the slope changed.

3.4. Discharge characteristics of Zn/MnO_2 cells in different types of electrolytes

In Leclanché cells it was found that the concentration of NH_4Cl controls the nature of the product, $Zn(NH_3)_2Cl_2$ or $ZnCl_2 \cdot 4Zn(OH)_2$ [253 - 255] (eqns. (1) and (2)), the latter being a monohydrate [256, 257]. The compositional changes in reactants and in products, as well as changes in potentials and in pH, occurring during cathodic reduction in Leclanché-type batteries have been summarized by Tye [258] (see Fig. 2). The changes are considered to occur in three stages. Initially, A - B, $Zn(NH_3)_2Cl_2$ is formed by consumption of NH_4Cl, the concentration of which is maintained

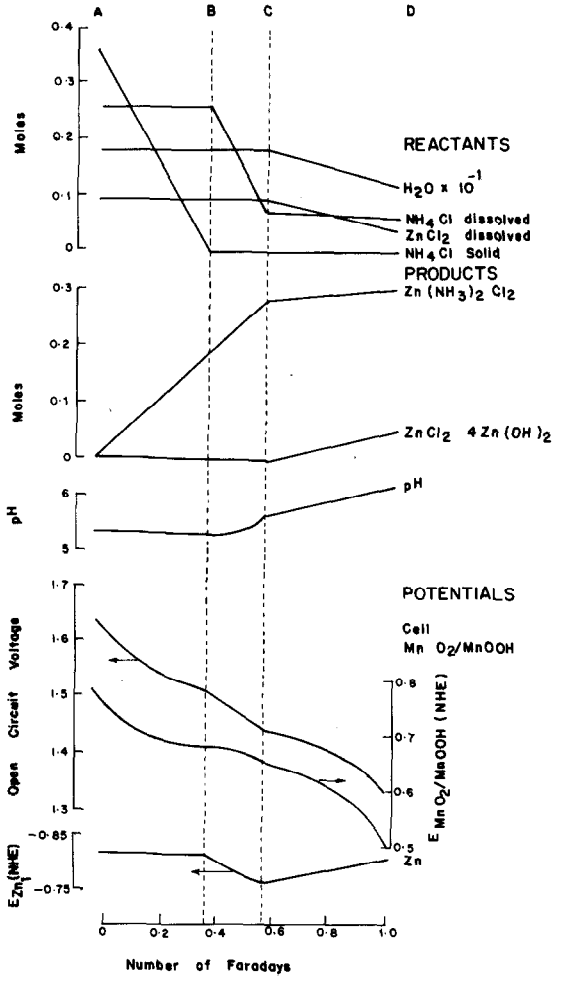

Fig. 2. Calculated composition and potential changes during slow discharge of Leclanché cells.

at its original value by shifting the saturation equilibrium $NH_4Cl(s) \rightleftharpoons NH_4Cl$ (dissolved) to the right. In the second stage, B - C, when all solid NH_4Cl is used up, the ammonia complex formation decreases the NH_4Cl concentration, resulting in a gradual rise in the pH of the solution. In the final stage, C - D, the rise in pH results in the formation of $ZnCl_2 \cdot 4Zn(OH)_2$ by consumption of $ZnCl_2$ and H_2O.

The potential of the zinc electrode, which remains constant in the beginning, rapidly falls in the middle stage due to a shift to the left of the equilibrium

$$Zn^{2+} + 4Cl^- \rightleftharpoons ZnCl_4^{2-}$$

as the NH_4Cl concentration falls [259]. During discharge hetaerolite, $ZnO \cdot Mn_2O_3$, is yet another major compound to be identified, but the conditions of its formation and the stage of discharge at which it can be formed are still not clear. McMurdie *et al.* [255] showed that if the pH of a solution containing manganous ions and dissolved zinc species is increased in the presence of MnO_2, hetaerolite is formed by the reaction:

$$MnO_2 + Mn^{2+} + Zn^{2+} + 2H_2O \longrightarrow ZnO \cdot Mn_2O_3 + 4H^+$$

This reaction buffers the solution in the pH range between 4 and 5, which is lower than the pH values (5.5 - 6.5) at which $Zn(NH_3)Cl_2$ and $ZnCl_2 \cdot 4Zn(OH)_2$ are precipitated. The net effect is the gradual dissolution of the latter with the subsequent regeneration of $ZnCl_2$ and NH_4Cl [185]. Thus,

$$ZnCl_2 \cdot 4Zn(OH)_2 + 8H^+ + 8Cl^- \longrightarrow 5ZnCl_2 + 8H_2O$$

is followed by the dissolution of $Zn(NH_3)_2Cl_2$:

$$Zn(NH_3)_2Cl_2 + 2H^+ + 2Cl^- \longrightarrow ZnCl_2 + 2NH_4Cl$$

Mn^{2+} ion formation in the electrolyte during discharge seems to be a prerequisite for hetaerolite formation; the former can be obtained from the reaction

$$MnOOH + H_2O + e^- \longrightarrow Mn^{2+} + 3OH^-$$

The above equation suggests that for hetaerolite formation during discharge the average value of r in $MnOOH_r$ should approach unity. This condition is usually satisfied after the end of one-electron reaction or at high current drains during the early part of discharge when the rate of proton diffusion in the MnO_2 lattice cannot keep up with the rate of formation of MnOOH at the MnO_2 surface. Recently, Uetani *et al.* [260] suggested the following reaction to account for the overall changes occurring during discharge of zinc chloride/Leclanché cells:

$$8MnO_2 + 4Zn + (l + 6n)ZnCl_2 + 8(l + n)H_2O \downarrow$$
$$4nMnO_2 + 8lMnOOH + 4nMnCl_2 + (l + 2n)ZnCl_2 \cdot 4Zn(OH)_2 + 4mMn_2O_3 \cdot ZnO$$

where $(l + m + n) = 1$, n is evaluated from the knowledge of Mn^{2+} formed in the electrolyte at a particular stage of discharge and m can be obtained from the amount of hetaerolite formed. It was found that l, m and n take different values during discharge and are different for electrolytic, chemical and natural manganese dioxide. In this way the relative discharge characteristics of different types of manganese dioxide could be readily understood.

The lowering of the open-circuit voltage with discharge of MnO_2 batteries represents polarization or discharge over-potential. It is the difference between the steady state open-circuit voltage obtained after discharge and the closed-circuit voltage at the end of the particular discharge

period. In general, the potential drop is very large during the initial stage of discharge and becomes smaller with increasing depth of discharge, when the potential does not recover its initial value even after time is allowed for recuperation. Neither the polarization due to the charge transfer process at the oxide solution interface nor the concentration polarization due to the pH change of the electrolyte alone could adequately account for the polarization [261, 262] and it was attributed to the accumulation of the lower oxide on the MnO_2 surface. It represents the concentration polarization within the solid oxide [263]. Yoshizawa studied the decay and the growth of polarization in acid, alkaline and neutral solutions [263, 264]. In acid solution the MnOOH formed by the reaction $MnO_2 + H^+ + e \rightarrow MnOOH$ was removed as fast as it was formed by the disproportionation process:

$$2MnOOH + 2H^+ \rightleftharpoons MnO_2 + Mn^{2+} + 2H_2O$$

The latter step was, therefore, the rate-determining one, as it then promoted the diffusion of protons and electrons within the lattice. The rapid removal of the lower oxide explained the constancy of the open-circuit voltage during discharge in acid solution. The acid electrolyte batteries, therefore, have very high discharge capacity which increases with acid concentration, with the load (pressure) on cathode mixtures and at low discharge current [265]. These merits are partly offset by dissolution of MnO_2 with increasing acidity [266], especially during storage, and by the presence of carbon which can act as a catalyst for MnO_2 dissolution [267].

In alkaline electrolyte, the hydroxyl ions generated by the charge transfer reaction ($MnO_2 + H_2O + e^- \rightarrow MnOOH + OH^-$) are not removed by a subsequent chemical reaction. However, the high mobility of hydroxyl ions, both in electrical transference and concentration diffusion, means that the concentration perturbation at the interface is very small [268]. There is, therefore, a considerable growth of polarization. The decay of polarization is brought about by the subsequent diffusion of protons into the lattice which is the rate-determining step in alkaline solution. δ-MnO_2 and Mn_3O_4 have been identified as the major discharge products at various depths of discharge [269] and their presence at any stage of discharge depends upon the type of MnO_2 involved.

Recently, Kanoh *et al.* [270] studied the discharge characteristic of α and γ forms of MnO_2 (chemically precipitated) in aqueous solutions of $ZnCl_2/NH_4Cl$ (at various concentrations and containing some HCl) by both continuous and intermittent discharge tests. The following reaction has been proposed for the overall cathodic reduction process:

$$MnO_2 + (1 - \epsilon)H_2O + \epsilon H^+ + e^- \longrightarrow \tfrac{1}{2}\epsilon Mn^{2+} + \tfrac{1}{2}\epsilon MnO_2^* + (1 - \epsilon)MnOOH + OH^-$$

ϵ denotes the rate of disproportionation contributed to the removal of MnOOH and is determined as the ratio of Mn^{2+} formed in the electrolyte at an equilibrium state to the theoretical value obtained from the reaction

$$MnO_2 + H_2O + e^- \longrightarrow \tfrac{1}{2}Mn^{2+} + \tfrac{1}{2}MnO_2^* + 2OH^-$$

$\epsilon = 1$ indicates that the reduction rate of MnO_2 by proton–electron insertion corresponds to the formation rate of Mn^{2+} by the above equation. The changes of the value of ϵ at various stages of discharge could explain the observed nature of the discharge curves. In neutral solutions of NH_4Cl, Yoshizawa [264] showed that the discharge over-potential is lowered by disproportionation carried out by NH_4^+ ions which act as proton donors. Thus:

$$2MnOOH + 2NH_4^+ \rightleftharpoons MnO_2 + Mn^{2+} + 2NH_3 + 2H_2O$$

The presence of Zn^{2+} further lowers the over-potential. The process involves the removal of NH_3 to form $[Zn(NH_3)_n]^{2+}$, thus preventing the pH rise which could occur by the reaction $NH_3 + H_2O \rightleftharpoons NH_4^+ + OH^-$, and which would otherwise have decreased the observed potential. Recently, Kozawa and Powers [208] determined the polarization values of I.C. MnO_2 samples both in 25% $ZnCl_2$ + 5% NH_4Cl solution and 9 M KOH solution at 1 mA discharge currents. In the former solution, the magnitude of polarization was almost twice that in KOH solution. The difference was found to be due to the pH change in the fine pores whose structure was mainly responsible for the observed magnitude of polarization [271]. At very low current discharge (0.1 mA), however, the values of polarization are almost the same in both types of solution [19]. Many times larger polarization values are obtained in solutions of NH_4Cl if they are poorly buffered. The buffer capacity of the solutions can, however, be considerably increased by the addition of 5% - 25% $ZnCl_2$ [272].

The increase in the open-circuit potential observed after washing the MnO_2 powder with 9 M - 10 M H_2SO_4 at 80 - 95 °C for several hours is attributed to the formation of manganate and the consequent existence of the MnO_2–MnO_4^{2-} system [273].

3.5. Electrochemical activity

A manganese dioxide which gives maximum energy with as high a cell voltage as possible is the most electrochemically active [218]. Many physical and chemical properties such as electrical conductivity, porosity, MnO_2 content, surface area, electrode potential, etc. have been measured and discussed in terms of dry cell performance. The combination of these factors which renders a given sample of MnO_2 most active, however, has been in question for years [219]. Brenet and co-workers in 1975 [73] were amongst the earliest to attempt any meaningful correlations between these factors. They established the importance of a large number of pores with mean radii between 15 and 24 Å as well as the existence of large amounts of OH groups in highly active dioxides. Subsequently, Kanungo *et al.* [219], in a similar study, suggested that the activity of an MnO_2 is determined by the type of OH groups present and the mobility of oxygen in the MnO_2 lattice. Voinov [274] explained the relative superiority of the γ-manganese dioxides

compared to the α and β forms on the basis of the proton insertion in the tetrahedral sites of the hexagonal close-packed oxygen layers. The presence of some of the tetrahedra which share no faces with the octahedra in a diaspore-type structure (γ-MnO_2, ramsdellite) was believed to favour proton diffusion (from the tetrahedral site to the other via an intermediate octahedral site). This effect is reinforced by lattice distortions which occur in a diaspore-type structure. Such an interpretation may be visualized as a simple diffusion of MnOOH or protons into the interior of the lattice, as was first recognized intuitively by Coleman [275].

The diffusion of MnOOH limits the capacity of MnO_2-based batteries. The diffusion of protons and electrons in electrodeposited MnO_2 is considered to be sufficiently fast for the manganese oxyhydroxide surface not to approach saturation in MnOOH until the bulk composition approaches MnOOH, *i.e.* until the capacity yield is close to 100% [276]. High current drains can lead to rapid surface saturation with MnOOH with no complementary compensation by diffusion into the interior. The diffusion process is facilitated by an increase in the surface area, which may explain some of the correlation between the battery activity of a dioxide and its surface area [75, 277]. Studies of Yoshizawa [263] indicated that the discharge capacity of EMD samples increased with the increasing intensity of the d_{110} X-ray peak. Recent studies of Fernandes *et al.* [75] showed that the electrochemical activity of the manganese dioxides is directly related to both the intensity of the 100 intensity X-ray peak and the H^+ ion exchange capacity of the OH groups. Fernandes *et al.* [75] also emphasized that the various crystalline forms of MnO_2 and their intermediates, all similarly prepared using the same chemical reaction, should be studied, so that a theoretical model which could predict *a priori* the experimentally observed behaviour of the dioxides could be evolved.

The practical evaluation of electrochemical (or battery) activity is as complex a situation as the concept of activity itself; capacity depends upon a number of factors such as:

(a) the type of battery, *i.e.* acid, alkaline or neutral electrolytes;

(b) structural and dimensional features of the cathode and its porosity;

(c) the quantity of the active dioxide which can be incorporated, depending upon the battery size, and the "tap" density* of the dioxides;

(d) the heat treatment, storage and shelf life, etc.

Another important aspect is how the MnO_2 battery is eventually used; the capacity yield depends upon the type of discharge regime. Various industrial specifications are in use, such as the *American National Standard* [278] and the *IEC* (International Electrotechnical Commission) *Recommendation* [279]. Some examples of the common discharge regimes, which depend on the size and type of the cell concerned, for meaningful evaluation of manganese dioxide dry cell batteries are as follows:

*"Tap" density is defined as the apparent density of a powder loosely compacted in a graduated cylinder before the volume is determined.

(1)	Heavy duty (*e.g.* motor)	4 Ω	high intensity flash test (HIFT) (15 min/h, 8 h/day)
		5 Ω	2 h/day
(2)	Medium duty (*e.g.* flash light)	10 Ω	4 h/day
		4 Ω	light intensity flash test (LIFT) (4 min/h, 8 h/day)
		5 Ω	30 min/day
(3)	Low duty (*e.g.* transistor radio)	40 Ω	4 h/day

These tests are usually carried out by constructing dry cells. Due largely to the efforts of Dr. Kozawa (Chairman of the I.C. MnO_2 Sample Office, Cleveland, Ohio, U.S.A.), a large variety of MnO_2 samples is available for evaluation in fundamental research and as standards for comparison with dioxides obtained from other sources. Various application tests carried out with I.C. MnO_2 samples confirmed the general superiority of the electrolytic manganese dioxides over the chemical ones, especially under heavy duty tests [280, 281]. The former are also invariably used for alkaline Zn/MnO_2 cells, mainly on account of their high open-circuit voltage [282], though there are recent reports on chemical MnO_2 samples exhibiting high open-circuit potentials in alkaline solutions [218]. Brenet *et al.* [283] recently related the cation exchange properties of the dioxides to their electrochemical activity. The observed deleterious effect of the divalent cations on discharge capacity in heavy duty tests was attributed to the blocking of pores for proton diffusion due to either —O—M—O— links across the pore, or to proton repulsion at —O—M^+ linkage which can exist at the pore walls by H^+ ion exchange of the OH groups. The less adverse effect of Zn^{2+} is due to its removal by complexing with ammonia in $ZnCl_2/NH_4Cl$ electrolyte cells. It is also interesting to note that a mixture of active, or activated ores, in combination with EMD or CMD exhibit synergistic effects, *i.e.* a higher discharge performance than theoretically expected [218, 284, 285].

Fabrication of commercial-type dry cells for testing is difficult, time consuming and requires a large amount of MnO_2. Various laboratory methods have been devised for rapid evaluation of the quality of the manganese dioxides under simulated battery conditions. Recently Kanungo *et al.* [219] reviewed some of the earlier methods. In general, they are of two types:

(i) depositing a thin film of MnO_2 on a conducting electrode material (such as graphitized polythene, graphitized foil, platinum or gold foil) and discharging it in a suitable electrolyte, usually NHCl and/or $ZnCl_2$, sometimes in the presence of additives [286 - 290] or incorporating the cathode mix in a perforated lead foil and discharging it in H_2SO_4 [291];

(ii) mixing the MnO_2 with acetylene black or graphite and pressing it into a pellet [240, 292 - 299].

Each of the methods seems to have its own merits and demerits, especially with regard to the simplicity of fabrication and the reproducibility of the results. Kanungo *et al.* [219] introduced a modified form of the method of Appelt and Purol [292], which makes use of a flowing electrolyte to flush the electrode during discharge.

The cell fabrication seems to be simple and is claimed to give reproducible results. The method given by Kozawa [299] is also relatively simple and involves discharging the cathode mix at 1 mA (0.1 g MnO_2 + 1 g graphite + 0.4 ml electrolyte) in 9 M KOH electrolyte. The cell voltages could be measured either with reference to Hg/HgO or Zn electrodes. The method has been used recently in a slightly modified form [218] and reproducible results were obtained. Discharging in 9 M KOH solution has an added advantage in that it involves no polarization due to pH change. The 'intrinsic' polarization, which is mainly concerned with the diffusion of protons in the MnO_2 lattice, can be obtained directly. The relative merits of different manganese dioxides are easily recognized. The main parameters to be evaluated are:

(i) open-circuit voltate at 5 mA h discharge

(ii) polarization at 5 mA h discharge, and

(iii) discharge at 1.0 V cut-off [299].

Any interpretation of the results should however, take into consideration the "tap" density of the dioxides as it may lead to an over-estimation of the less dense manganese dioxides.

3.6. Rechargeability of alkaline MnO_2/Zn cells

Kang and Liang [300] were amongst the earliest to attempt to recharge alkaline MnO_2/Zn cells. They showed that the efficiency of anode oxidation is a function of the KOH cencentration: the efficiency decreases as the KOH concentration increases from 1 M to 10 M KOH. The current density used for the discharge ranged from 0.2 to 2 mA/cm^2 (of apparent surface area) and did not affect the electrochemical behaviour.

Boden and co-workers also investigated the charge process of MnO_2 in alkaline electrolyte [301]. However, they kept the concentration of KOH constant at 7 M and concluded that the electrode was rechargeable in the early stage of discharge. The existence of an amorphous phase of MnO_2 was also postulated, which reduces to Mn_3O_4 at greater depth of discharge. Once the Mn_3O_4 formed, it was practically impossible to recharge. The charge–discharge reaction they proposed is as follows:

$$MnO_2 + nH^+ + ne^- \longrightarrow MnO_{2-n}(OH)_n \qquad (14)$$

or

$$MnO_2 + nH_2O + ne^- \longrightarrow MnO_{2-n}(OH)_n + n(OH)^- \qquad (15)$$

The quantity of electricity discharged was found to be almost equal to the amount needed to recharge above $MnO_{1.55}$. The diffraction peaks of Mn_3O_4 were detected from $MnO_{1.46}$ onwards. Electrodes discharged to greater depths (*e.g.* to $MnO_{1.29}$) showed a rapid rise of charge voltage and a large amount of Mn_3O_4.

Ohira and Ogawa [302] determined the cycle life as a function of the depth of discharge in 7 M KOH. They obtained 30 cycles at 30% depth of discharge to −0.25 V against HgO. Miyazaki [303] explained the relative charge–discharge behaviour of MnO_2 both in Leclanché and in alkaline batteries and described the mechanism involving injection of K^+ and Zn^{2+} ions into the MnO_2 lattice. It is obvious that the rechargeability of alkaline MnO_2 is far superior to that of Leclanché cells. McBreen [304] used cyclic sweep voltametry for testing the rechargeability of MnO_2 electrodes. He showed the poor rechargeability of deep-discharged MnO_2. Kordesch and Gsellmann [305] delineated the criteria for the rechargeability of alkaline MnO_2 batteries which are important to both battery technologists and electrochemists. Some of these criteria are as follows.

(1) MNO_2 electrodes can only be discharged to one-third capacity of 0.3 A h g^{-1} in order to remain rechargeable.

(2) The rechargeability of Zn electrodes in alkaline electrolytes has been established but gives satisfactory results only if its capacity is more than twice that of the cathode. This does not seem feasible unless other precautions are taken.

(3) The cells must be hermetically sealed and made safe for use under abusive conditions without making the cost too great.

(4) The addition of good binders, improved technical strength and thin layer structure are equally important.

(5) The collector should be coated with a conducting paint of MnO_2/graphite.

(6) The upper voltage limitation on charge is important. On over-charge, the soluble manganate Mn(VI) occurs, which constitutes a capacity loss and leads to corrosion problems.

(7) In a rechargeable cell with a membrane separator, steps must be taken for free oxygen movement in the anodic compartment so that ZnO forms and prevents the pressure build-up beyond a safe limit.

Kordesch and Gsellmann also concluded that, with a relatively small effort in cell design, the primary alkaline MnO_2/Zn cells could easily be converted to rechargeable ones. The benefits certainly outweigh the added costs that will accrue. Both high and low temperature performance of the MnO_2/Zn cell is good, and therefore every effort should be made to make it cost-effective.

Subsequently, Kordesch and co-workers [306] gave details of rechargeability and the optimum conditions necessary to get satisfactory results. In order to determine dimensional changes of the MnO_2 (disc contraction and expansion), they used two types of electrode. One cathode was mounted on a steel cap (such that it was confined), and the other

on a flat plate with a slight pressure to ensure contact but freedom to expand. Their results are shown in Fig. 3. It is obvious that the behaviour of a confined electrode was different from that of a free electrode. Bulging and mechanical disintegration terminated one of the experiments after four cycles, while the other continued, and appeared to reach equilibrium. A small loss of capacity was observed as cycling continued.

This experiment, according to the authors, explains why cylindrical cells with sleeve cathodes (such as LR-20 LR-14, LR-16, alkaline MnO_2/Zn cells) are rechargeable until either the zinc or the separator fails. The failure is not due to build-up of an insulating layer, but a mechanical disintegration accompanied by a resistance increase. They carried out the subsequent tests with a special cell assembly [307] to allow for these mechanical problems. One of the important conclusions was that the number of cycles depended on the depth of discharge (DOD). The analytical expression given by Voss and Huster seems to apply well to this relationship [308]:

$$\log (\text{No. of cycles}) = (A - B)\,\text{DOD} \quad (\%)$$

When $A = 3$, and $B = 0.04$ and with a 35% DOD, the number of cycles was 39; for a 20% DOD, it was 128 (see Fig. 4).

It was also noticed that cycling led to the deposition of a material which was a poor conductor. No correlation, however, was found between the cycling data and the physical properties of I.C. samples and their primary discharge capacity at 35% depth of the one-electron discharge reaction. The number of cycles obtained for various I.C. MnO_2 samples in relation to their primary discharge capacity is shown in Table 1.

Kordesh and co-workers also reported [306] that with commercial LR-14 MnO_2/Zn alkaline cells built with the best I.C. samples, the rechargeability was as good as reported, and in some cases even better than expected.

To incorporate the principle that commercial cells must be Zn-limited to be fool-proof against discharge beyond the one-electron limit, it is possible

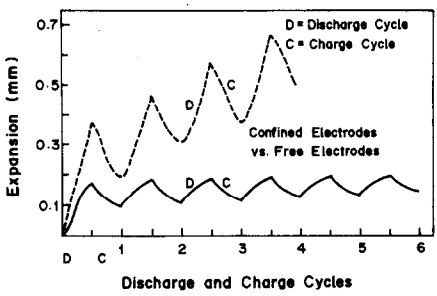

Fig. 3. The perpendicular expansion and contraction of 3 mm thick MnO_2/graphite discs during cycling.

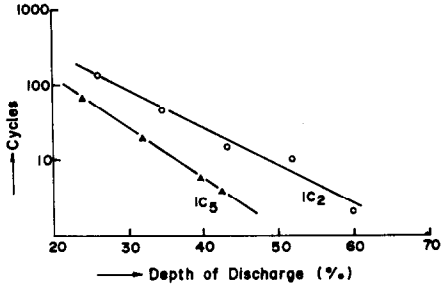

Fig. 4. The number of discharge–charge cycles as a function of the depth of discharge for samples of I.C. 2 (EMD) and I.C. 5 (CMD).

TABLE 1

Number of cycles obtained for various I.C. MnO_2 samples in relation to their primary discharge capacity

I.C. sample	1	2	3	4	5	8	9	10	11
No. of cycles	41	42	31	38	20	31	29	40	31
Primary discharge capacity	84	86	82	89	83	79	56	73	70

to redesign the cells with more MnO_2 than regular primary cells of the same size. This could lead to a 15% - 25% range of depth of discharge, thus leading to the higher cycle life of the MnO_2 electrode of 100 - 200 cycles. A remarkable increase in charge–discharge characteristics has been observed when MnO_2 is mixed with nickel oxyhydroxide [309].

Summary of electrochemical properties

Over the years many models have been proposed which could account for the observed discharge behaviour of manganese dioxides both in acidic and alkaline electrolytes. An elegant model, proposed by Atlung and Jacobsen [229], seems, in the words of Tye [310], "to be rather unreal though ingenious". Further, Tye [311], in his quest for a better model, has proposed a more realistic version which satisfactorily explains the distinct change in potential *versus* r slope at the mid-reduction point. It would be interesting to examine the applicability of the model to the discharge characteristics of various electrochemically active MnO_2 polymorphs.

4. Conclusion

In spite of intensive research for more than a hundred years, the MnO_2/Zn battery system is still a "black art" in the words of Atlung and Jacobsen [229]. There are several reasons for this. One of the important ones is that the research work conducted by the industry is often either not published or only published in a truncated form for commercial reasons. On the academic side there is a general view that "MnO_2 is a very complicated material; one really cannot put one's finger on all parameters, neither can they be simplified or controlled reasonably enough; no single crystals could be grown easily; ...". The laws of nature do not seem to hold in any case. As a result, these attitudes, and the problems that arose out of them, have hindered the development of a comprehensive knowledge of MnO_2/Zn battery systems. As has been stated [75] no theoretical model has yet immerged enabling one to determine *a priori* the performance of a given MnO_2 or the type of MnO_2 required for a particular battery system. Also, no theory connecting all variables such as structure, surface area, pore size and shape, particle size, pH–potential behaviour and hydroxyl groups present has yet evolved. Largely due to the efforts of the I.C. MnO_2 Sample Office of

Cleveland, Ohio, U.S.A., in bringing together both battery technologists and electrochemists, much progress has been made of late. Still, a great deal needs to be done to successfully substitute experience and intuition by a sound scientific knowledge so that battery-making does not remain a "black art".

Acknowledgements

We are indebted to Dr. Pierre Chartier, Laboratoire d'Electrochimie et Chimie Physique des Corps Solides, Université Louis Pasteur, Strasbourg, France, for having extended generous financial help to one of us (B.D.D.) during his stay in his laboratory to retrieve the literature from the computer data bank. We are also grateful to A. Kozawa, Chairman of the I.C. MnO_2 Sample Office, Cleveland, OH, U.S.A., F. L. Tye of the Energy Technology Centre, Middlesex Polytechnic, London, U.K., and K. V. Kordesch, Technical University of Graz, Austria, for kindly allowing us to include Figs. 1, 2 and 3 respectively.

List of symbols

a	Activity
B	Magnetic induction
E	Electrode potential
E^0	Standard electrode potential
E^θ	Sum of standard electrode potential and other constants
$\bar{E}$	Potential corrected for pH
e^-	Electron
F	Faraday constant
ΔG	Gibbs free energy charge
I	Intensity of 100 X-ray peak
J	Exchange integral
J_1	Exchange integral between nearest neighbours in (001) direction
J_2	Exchange integral which acts between next-nearest neighbours in (111) direction
J_3	Third exchange integral between (100) or (010) neighbours
k	Boltzmann's constant
m	Mole concentration of combined water in MnO_2
R	Gas constant
R_H	Hall coefficient
r	Degree of reduction
S	Vector sum of spin moments
T	Absolute temperature

$t_{\parallel}$	Localized electrons having spin axis in (111) direction
$t_{\perp}$	Localized electrons having spin axis in (001) direction
X	Mole fraction
z	Co-ordination number
$\alpha, \beta, \gamma, \delta, \epsilon, \mu, \rho$	Various MnO_2 polymorphs
Δ	Weiss constant
μ	Reduced mass
μ_B	Bohr magneton
μ_e	Electrochemical potential for insertion of electron
μ_{Mn}	Atomic moment
$\bar{\nu}$	M–O stretching frequency
π^*, σ^*	Antibonding orbitals
σ	Electrical conductivity
χ	Magnetic susceptibility
ψ	Spatial correlation coefficient

References

1 J. P. Brenet, *J. Power Sources, 4* (1979) 183 - 190.
2 E. Preisler, *J. Appl. Electrochem., 6* (1976) 301 - 320.
3 V. G. Bhide and R. V. Damle, *Physica, 26* (1960) 33 - 42.
4 V. I. Gryaznov, *Dokl. Akad. Nauk SSSR, 121* (1958) 159.
5 J. S. Wiley and H. T. Knight, *J. Electrochem. Soc., 111* (1964) 659 - 660.
6 K. Sasaki and K. Kozawa, *J. Electrochem. Soc. Jpn., 22* (1954) 564.
7 J. P. Brenet, *Croat. Chem. Acta, 44* (1972) 115.
8 P. H. Klose, *J. Electrochem. Soc., 117* (1970) 854 - 858.
9 J. N. Das, *Z. Phys., 151* (1958) 345.
10 V. G. Bhide and R. H. Dani, *Physica, 27* (1961) 821.
11 S. Yu. Elovich and Ya. Margolis, *Dokl. Akad. Nauk SSSR, 107* (1956) 112; *Chem. Abstr., 50* (1956) 15192d.
12 J. P. Brenet, *C.R. Acad. Sci., 247* (1958) 783.
13 J. P. Chevillot and J. P. Brenet, *C.R. Acad. Sci., 249* (1959) 1869.
14 P. Lançon, J. P. Chevillot and J. P. Brenet, *C.R. Acad. Sci., 258* (1964) 6411.
15 J. P. Brenet, *Chem.-Ing.-Tech., 38* (1966) 658.
16 J. B. Foster, J. A. Lee and F. L. Tye, *J. Appl. Chem. Biotechnol., 22* (1972) 1085.
17 J. M. Honig, *J. Chem. Educ., 43* (1966) 76.
18 K. J. Euler, *J. Power Sources, 3* (1978) 117 - 136.
19 J. McBreen, *MnO_2 Symp. Proc., Cleveland, OH, 1* (1975) 97 - 110.
20 R. Glicksman and C. K. Morehouse, *J. Electrochem. Soc., 103* (1956) 149 - 153.
21 L. Pons and J. P. Brenet, *C.R. Acad. Sci., 259* (1964) 2825; *260* (1965) 2483.
22 R. Kirchhof, *MnO_2 Symp. Proc., Tokyo, 2* (1980) 648.
23 K. J. Euler, *Metalloberfläche-Angew. Elektrochem., 28* (1974) 15 - 20.
24 K. J. Euler, *J. Appl. Electrochem., 9* (1979) 395 - 398.
25 K. J. Euler and T. Harder, *Electrochemistry, 26* (1981) 1661 - 1667.
26 K. J. Euler, R. Kirchhof and H. Metzendorf, *J. Power Sources, 5* (1980) 255 - 262.
27 K. J. Euler, *J. Power Sources, 7* (1981/1982) 95 - 102.
28 R. Kirchhof, *J. Power Sources, 4* (1979) 281 - 290.
29 K. J. Euler, *J. Power Sources, 4* (1979) 215 - 226.
30 K. J. Euler, *Mater. Chem., 4* (1979) 611 - 630.
31 S. R. Broadbent and J. M. Hammersley, *Proc. Cambridge Philos. Soc. Mater. Phys. Sci., 53* (1957) 629 - 641.

32 P. Herger, *Diss.*, Gesamthochschule Kassel, F.R.G., 1978.
33 D. A. G. Bruggeman, *Ann. Phys. (Leipzig), 24* (1935) 636 - 664.
34 D. Adler, I. P. Flora and S. D. Senturla, *Solid State Commun., 12* (1973) 9 - 12.
35 P. Ruetschi, R. Giovanoli and P. Burki, *MnO_2 Symp. Proc., Cleveland, OH, 1* (1975) 12.
36 A. Vosekalns, G. Slaidins and M. Kuzmane, *Latv. PSR Zinat. Akad. Vestis, Kim. Ser., 3* (1978) 375 - 376.
37 K. J. Euler, *Naturwissenschaften, 67* (1980) 561 - 562.
38 B. I. Kachibaya and L. N. Dzhaparidze, *Izv. Akad., Neuk Gruz. SSR, Ser. Khim., 7* (1981) 345 - 349.
39 J. M. Albella, L. N. Fernandez and J. M. D. Martines, *J. Appl. Electrochem., 11* (1981) 273 - 279.
40 A. S. Syed, N. Morshed, A. S. Haider, F. A. Majumdar and S. A. Islam, *Prog. Batteries Sol. Cells, 4* (1982) 132 - 137.
41 K. J. Euler and H. M. Helsa, *J. Power Sources, 4* (1979) 77 - 89.
42 H. Mueller, *Electrochim. Acta, 23* (1978) 1093 - 4.
43 J. Brenet and P. Faber, *J. Power Sources, 4* (1979) 203 - 213.
44 K. Honda and T. Sone, *Sci. Rep. Tohoku Imp. Univ., Ser. 1, 3* (1914) 139.
45 R. W. Taylor, *Phys. Rev., 44* (1933) 776.
46 H. Bizette, C. P. Squire and B. Tsai, *C.R. Acad. Sci., 207* (1938) 449.
47 S. S. Bhatnagar, A. Lamerson, E. H. Harbard, P. L. Kapoor, A. King and B. Prakash, *J. Chem. Soc.*, (1939) 1433.
48 J. Amiel, J. P. Brenet and G. Rodier, *Proc. Conf. on the Polarization of Matter, Paris, April 4 - 9, 1949.*
49 P. W. Selwood, M. Ellis and C. F. Davis, *J. Am. Chem. Soc., 72* (1950) 3549.
50 T. Moore, M. Ethes and P. W. Selwood, *J. Am. Chem. Soc., 72* (1950) 856.
51 M. Faraday, *Experimental Researches in Electricity, Ser. 3*, 1855, para. 22 497.
52 P. W. Selwood, *J. Am. Chem. Soc., 61* (1939) 3168.
53 P. W. Selwood, R. P. Eischens, M. Ellis and K. Wellington, *J. Am. Chem. Soc., 71* (1949) 3039.
54 K. M. Parida, S. B. Kanungo and B. R. Sant, *Electrochim. Acta, 26* (1981) 435.
55 H. Bizette and B. Tsai, *Proc. Conf. on the Polarization of Matter, Paris, April 4 - 9*, 1949.
56 J. T. Grey, *J. Am. Chem. Soc., 68* (1946) 605.
57 L. Pauling, *Phys. Rev., 54* (1938) 899.
58 J. Brenet, *J. Chim. Phys., 46* (1949) 597.
59 M. C. Baird, *Prog. Inorg. Chem., 9* (1968) 1.
60 J. Amiel, R. Rodier and J. Brenet, *C.R. Acad. Sci., 227* (1948) 1356.
61 P. W. Selwood, *Magnetochemistry*, Interscience Publishers, New York, 1943; *J. Am. Chem. Soc., 69* (1947) 1590.
62 J. B. Goodenough, *Bull. Soc. Chim. Fr.*, (1965) 1200.
63 J. Brenet, *Chem.-Ing.-Tech., 38* (1966) 658 - 660.
64 J. B. Goodenough, *Prog. Solid State Chem., 5* (1978) 214.
65 A. Yoshimori, *J. Phys. Soc. Jpn., 14* (1959) 807 - 821.
66 R. A. Erickson, *Phys. Rev., 90* (1953) 779.
67 S. L. Strong, *Physics Chem. Solids, 19* (1961) 51; *Chem. Abstr., 60* (1964) 1447h.
68 O. V. Kovalev, *Fiz. Tverd. Tela, 7* (1965) 103; *Chem. Abstr., 62* (1965) 1230d.
69 W. P. Osmond, *Proc. Phys. Soc., 87* (1966) 335.
70 S. Ghosh and J. Brenet, *Ber. Bunsenges. Phys. Chem., 67* (1963) 723.
71 P. W. Selwood, *Magnetochemistry*, Interscience, New York, 2nd edn., 1956.
72 J. Labat and J. P. Gabano, *C.R. Acad. Sci., Ser. C, 264* (1967) 164.
73 J. P. Brenet, M. Cyrankowska, G. Ritzler, R. Saka and K. Traore, *MnO_2 Symp. Proc., Cleveland, OH, 1* (1975) 264 - 268 (retyped text).
74 J. P. Brenet, K. Traore and J. P. Kappler, *MnO_2 Symp. Proc., Cleveland, OH, 1* (1975) 290 - 297 (complement to above article, retyped text).

75 J. B. Fernandes, B. D. Desai, V. N. Kamat Dalal, *Electrochim. Acta, 29* (1984) 187.
76 J. B. Fernandes, B. D. Desai, V. N. Kamat Dalal, *J. Appl. Electrochem, 15* (1985) 351 - 363.
77 J. B. Fernandes, *Ph.D. Thesis*, Unviersity of Bombay, 1983.
78 M. Parodi, *C.R. Acad. Sci., 20* (1937) 205.
79 G. Gattow and O. Glemser, *Z. Anorg. Allg. Chem., 309* (1961) 20 - 21.
80 R. M. Veletta and W. A. Pliskin, *J. Electrochem. Soc., 114* (1967) 9, 944.
81 J. V. Valarelli, M. Perrier and G. Vincente, *An. Acad. Bras. Cienc., 40* (1968) 289.
82 J. M. Grey and A. P. Millmann, *Econ. Geol., 57* (1962) 325.
83 R. E. Folino, *Econ. Geol., 44* (1949) 425.
84 E. M. Shazly and G. S. Saleeb, *Econ. Geol., 54* (1959) 873.
85 O. Glemser, G. Gattow and H. Meisick, *Z. Anorg. Allg. Chem., 309* (1961) 1.
86 G. A. Kotla, F. M. A. Kerim and A. A. A. Azin, *Z. Anorg. Allg. Chem., 384* (1971) 260.
87 P. Faber, *Ph.D. Thesis*, Université Louis Pasteur, Strasbourg, France, 1976.
88 R. M. Valetta, J. Makris and G. Vincenti, *Proc. Electron. Comp. Conf.*, 1966.
89 N. T. McDewitt and W. L. Baun, *Spectrochim. Acta, 20* (1964) 799.
90 O. Henning and U. Strobel, *Wiss. Z. Hochsch. Archit. Bauwes. Weimar, 14* (1967) 645.
91 *IR-Tabellen*, Sadtler Res. Lab. Inc., Philadelphia, U.S.A., 1965.
92 E. A. Yanchuk and A. S. Povarennyk, *Mineral. Sb. (Lvov), 30*(2) (1976) 9.
93 K. P. Zhdanova, A. V. Panikarovskaya and N. V. Alekseeva, *Katal. Prevrashchenia Uglevadorodov Irkutsh*, (1980) 45.
94 P. Faber, *Chem.-Ing.-Tech., 49* (1977) 333.
95 A. Kozawa, *MnO_2 Symp. Proc., Cleveland, OH, 1* (1975) 499.
96 W. B. White and R. Roy, *Am. Mineral., 49* (1964) 1670.
97 J. P. Brenet and P. Faber, *Symp. ISE Batteries, Marcoussis, France, May 1975.*
98 J. B. Fernandes, B. Desai and V. N. Kamat Dalal, *Electrochim. Acta, 28* (1983) 309.
99 O. Glemser and E. Hartert, *Z. Anorg. Allg. Chem., 283* (1956) 11.
100 C. Gabannes, *Ann. Chim. (Paris), 5* (1960) 905.
101 D. Vivien, J. Livage and C. Maxienes, *J. Chim. Phys., 67* (1970) 199.
102 E. Narita and T. Okabe, *Bull. Chem. Soc. Jpn., 53* (1980) 525.
103 Chang Chi-Hsun, *MnO_2 Symp. Proc., Tokyo, 2* (1960) 543.
104 R. M. Potter and G. R. Rossman, *Ann. Mineral., 64* (1979) 1199.
105 D. M. Tinsley and J. H. Sharp, *J. Therm. Anal., 3* (1971) 43.
106 H. E. Kissinger, H. F. McMurdie and B. S. Simpson, *J. Am. Ceram. Soc., 39* (1956) 168.
107 R. C. McKenzie and G. Berggren, *Differential Thermal Analysis* Vol. 1, Academic Press, New York, 1970, Chap. 9.
108 D. Dollimore, *Differential Thermal Analysis*, Vol. 1, Academic Press, New York, 1970, Chap. 13.
109 D. Dollimore, *Proc. Soc. Anal. Chem.*, (1965) 167.
110 S. Palivitch, *C.R. Acad. Sci., 200* (1935) 71.
111 H. F. McMurdie and E. Golovato, *J. Res. Nat. Bur. Stand., 41* (1958) 145.
112 E. Ya. Rode, *Trans. 1st Conf. on Thermal Analysis, Karzam, 1955.*
113 A. J. Hegedus, *Magy. Chem. Foly., 72* (1966) 79.
114 L. K. Svanidze, T. I. Signa and M. A. Kakelidze, *V. Sb., Pererab. Zkelezn. i Margants Rud. Zakavk. 'Ya, 1975*, p. 71
115 S. Koshinaka and K. Higikata, Nippon Daigaku *Bunrigakubu Shizenkagaku Kenkyusho Kenkyu Kiyo, 12* (1977) 27.
116 D. S. Freeman, P. F. Pelter, F. L. Tye and L. L. Wood, *J. Appl. Electrochem., 1* (1971) 127.
117 P. D. Garn, *Thermoanalytical Methods of Investigation*, Academic Press, London, 1965, Chap. VII.
118 J. P. Gabano, B. Morigant, E. Fialdes, B. Emery and J. F. Laurent, *Z. Phys. Chem., 46* (1965) 359.

119 P. Brouillet, A. Grund, F. Jolas and R. Mellet, in D. H. Collins (ed.), *Batteries, 2* Pergamon Press, Oxford, 1965, p. 189.
120 N. S. K. Prasad and C. C. Patel, *Bull. India Sect. Electrochem. Soc., 12* (1963) 12.
121 J. Muller, F. L. Tye and L. L. Wood, in K. Takahashi, S. Yoshizawa and A. Kozawa, *Electrochemistry of Manganese Dioxide and Manganese Dioxide Batteries in Japan*, U.S. Branch Office, Electrochem. Soc. Jpn., Cleveland, OH, 1971, p. 201.
122 M. A. Dakri, F. L. Tye and J. L. Whiteman, in D. H. Collins (ed.), *Power Sources, 1966*, Pergamon Press, Oxford, 1967, p. 65.
123 K. Le Tran, *J. Chim. Phys., 64* (1967) 922.
124 S. Tobisawa, *Mem. Def. Acad. Math. Phys. Chem. Eng., 2* (1963) 97.
125 D. Dollimore and K. H. Tonge, *Reactivity of Solids*, Elsevier, Amsterdam, 1965, p. 497.
126 J. P. Brenet, J. P. Gabano and M. Siegneurin, *Proc. Int. Congr. Pure Appl. Chem., 9* (1957) 69 - 80; *Chem. Abstr., 54* (1960) 12859.
127 T. Matsushima and W. J. Thoburn, *Can. J. Chem., 43* (1965) 1723.
128 A. Kozawa, *J. Electrochem. Soc., 106* (1959) 552.
129 J. Koshiba and S. Nishizawa, *Nippon Koenchi Kogyokai*, (1971) 114.
130 M. Sato, K. Matsuki, E. Takaski and H. Yamamoto, *Yamagata Daigaku Kiyo Kogaku, 15* (2) (1979).
131 H. G. McAdie, *Anal. Chem., 39* (1967) 417.
132 P. D. Garn, *Thermoanalytical Methods of Investigation*, Academic Press, London, 1965.
133 H. F. McMurdie and E. Golovato, *J. Res. Nat. Bur. Stand., 41* (1948) 589.
134 J. L. Kulp and J. N. Perfetti, *Mineral. Mag., 29* (1950) 239.
135 B. L. Sreenivasan, *Mineral. Mag., 31* (1957) 605.
136 A. G. Dessai and G. G. Deshpande, *J. Mines Met. Fuels, 26*(5) (1978) 193.
137 L. Zawislak, *Thermal Analysis (Proc. 6th Int. Conf. on Thermal Analysis)*, Vol. 2, 1980, p. 307.
138 F. V. Foldvari and V. Koldencz, *Acta Univ. Szeged. Acta Miner. Petrogr., 9* (1956) 7.
139 G. Graselly and E. Klivengi, *Acta Univ. Szeged. Acta Miner. Petrogr., 9* (1956) 15.
140 R. D. Agrawal, *Trans. Jpn. Inst. Met., 22* (1981) 253.
141 D. Dollimore and K. H. Tonge, *Thermal Analysis (Proc. 3rd Int. Conf. on Thermal Analysis), 1971*, Vol. 2, 1972, pp. 91 - 103.
142 A. J. Hegedas and K. Harkey, *Microchim. Acta*, (1966) 453.
143 A. J. Hegedas, *Acta Chim. Acad. Sci. Hung., 46* (1965) 311.
144 G. Hahn and W. Dusdorf, *Acta Chim., 56* (1968) 99.
145 H. W. Fishburn Jr. and E. E. Dill Jr., *Proc. Am. Power Sources Conf., 15* (1961) 98.
146 L. Pons and J. Brenet, *C.R. Acad. Sci., 259* (1964) 2895.
147 K. Hochstrasser and W. Feitknecht, *Thermal Analysis (Proc. 3rd Int. Conf. on Thermal Analysis)*, Vol. 2, 1972, pp. 78 - 79.
148 M. Sato, K. Matsuki, E. Takashi and H. Yamamoto, *Yamagata Daigaku Kiyo Kogaku, 15*(2) (1979).
149 J. P. Brenet and A. Grund, *C.R. Acad. Sci., 240* (1955) 1210.
150 J. P. Brenet, A. Grund and F. Jolas, *Chem. Abstr., 51* (1957) 17547.
151 I. B. Foster, J. A. Lee and F. L. Tye, *Thermochim. Acta, 9* (1974) 55.
152 O. Glemser, G. Gattow and H. Meisick, *Z. Anorg. Allg. Chem., 309* (1961).
153 P. H. Delano, *Ind. Eng. Chem., 42* (1950) 523.
154 B. P. Varma, *MnO_2 Symp. Proc., Tokyo, 2* (1980) 256.
155 F. Paulik, J. Paulik and L. Erday, *Z. Anal. Chem., 160* (1958) 241.
156 E. Preisler, *MnO_2 Symp. Proc., Tokyo, 2* (1980) 184.
157 E. D. Jegge, *Trans. Electrochem. Soc., 53* (1928) 71.
158 K. Sasaki and A. Kozawa, *J. Electrochem. Soc. Jpn., 25* (1957) 115.
159 K. Sasaki and A. Kozawa, *J. Electrochem. Soc. Jpn., 25* (1957) 273.
160 M. Fukuda, *J. Electrochem. Soc. Jpn., 28* (1960) 67.

161 C. Drotschmann, *Modern Primary Batteries*, Nikolaus Branz, Berlin, 1951, pp. 38 - 39.
162 C. Drotschmann, *Batterien, 14* (1960) 49.
163 A. Kozawa, *J. Electrochem. Soc., 106* (1959) 839.
164 G. Gattow and O. Glemser, *Z. Anorg. Allg., Chem., 309* (1961) 1212; *309* (1961) 20.
165 O. Glemser and H. Meisick, *Naturwissenschaften, 44* (1957) 614.
166 O. Glemser, *Nature (Lond.), 183* (1959) 943.
167 A. Tvarusko, *J. Electrochem. Soc., 111* (1964) 125.
168 R. Huber and A. Schmier, *Electrochim. Acta, 3* (1960) 127.
169 K. Neuman and W. Fink, *Z. Elektrochem., 62* (1958) 114.
170 M. Kiriyama, *Kobutsugaku Zasshi, 7* (1964) 39; *Chem. Abstr., 64* (1966) 9107d.
171 R. F. Amlie and A. Tvarusko, *J. Electrochem. Soc., 111* (1964) 496.
172 F. L. Tye, *Electrochim. Acta, 21* (1976) 415.
173 J. A. Lee, C. E. Newnham and F. L. Tye, *J. Colloid Interface Sci., 42* (1973) 372.
174 J. A. Lee, C. E. Newnham, F. S. Stone and F. L. Tye, *J. Colloid. Interface Sci., 45* (1973) 289.
175 J. L. Hitchcock and P. F. Pelter, in I. Buzas (ed.), *Thermal Analysis (4th. Int. Conf. on Thermal Analysis) 1974*, Vol. 1, Heyden, London, 1975, pp. 979 - 989.
176 J. A. Lee, C. E. Newnham, F. L. Tye and F. S. Stone, *J. Chem. Soc., Faraday Trans. 1, 74* (1978) 237.
177 R. Giovanoli and U. Leuenberger, *Helv. Chim. Acta, 52* (1969) 2333.
178 A. Agopsowicz, J. L. Hitchcock and F. L. Tye, *Thermochim. Acta, 32* (1979) 63 - 71.
179 K. Miyazaki, *MnO_2 Symp. Proc., Cleveland, OH, 1* (1975) 111.
180 T. Yoshimori, M. Kato, K. Nippashi and J. Murayama, *MnO_2 Symp. Proc., Tokyo, 2* (1980) 369.
181 T. Yoshimori and N. Sakaguchi, *Talanta, 22* (1975) 233.
182 T. Yoshimori, Y. Asano and Y. Hattori, *Talanta, 26* (1979) 577.
183 T. Yoshimori, S. Ishiwari, Y. Watanabe and S. Yamoda, *Trans. Jpn. Inst. Met., 14* (1974) 396.
184 L. Erday, transl. by G. Svehla, *Gravimetric Analysis, Part 1*, Macmillan, New York, 1983, p. 298.
185 F. L. Tye, in M. Barak (ed.), *Primary Batteries for Civilian Use: Electrochemical Power Sources*, Peter Peregrinus, London, 1980, pp. 50 - 180.
186 J. P. Gabano, J. F. Laurent and B. Morignat, *Electrochim. Acta, 9* (1964) 1093.
187 G. S. Bell and R. Huber, *J. Electrochem. Soc., 111* (1964) 1.
188 M. Beley and J. P. Brenet, *Electrochim. Acta, 18* (1973) 1003.
189 J. P. Brenet, *Int. Comm. Electrochem. Thermodyn. and Kinetics (CITCE), Madrid, 1956.*
190 J. P. Brenet, P. Malessan and A. Grund, *C.R. Acad. Sci., 242* (1965) 111.
191 K. Neumann and W. Fink, *Z. Electrochem., 62* (1958) 114.
192 D. Boden, C. U. Venuto, D. Wisler and R. B. Wylie, *J. Electrochem. Soc., 114* (1967) 415.
193 J. P. Gabano, B. Morignat and B. F. Laurent, in D. H. Collins (ed.), *Power Sources, 1966*, Pergamon Press, Oxford, 1967, pp. 49 - 63.
194 J. McBreen, in D. H. Collins (ed.), *Power Sources 5*, Academic Press, London, 1975, pp. 523 - 534.
195 J. P. Gabano, B. Morignat, E. Fialdes and B. Emery, *Z. Phys. Chem., Abt. A, 46* (1965) 359.
196 W. Feitknecht, H. R. Oswald and U. Feitknecht-Steinmann, *Helv. Chim. Acta, 43* (1960) 1947 - 1949.
197 H. Bode, A. Schmier and D. Berndt, *Z. Elektrochem., 66* (1962) 586.
198 K. J. Vetter, *Z. Elektrochem., 66* (1962) 577.
199 H. Bode and A. Schmier, *3rd Int. Symp. on Batteries, Bournemouth, 1962.*

200 K. J. Vetter and N. Jaeger, *Electrochim. Acta, 11* (1966) 401; F. L. Tye, *Electrochim. Acta, 21* (1976) 415.
210 A. Kozawa and R. A. Powers, *J. Electrochem. Soc., 113* (1966) 870.
202 A. Kozawa, in J. Thompson (ed.), *Power Sources 7*, Academic Press, London, 1979, 485.
203 A. Kozawa and J. F. Yeager, *J. Electrochem. Soc., 115* (1968) 1003.
204 A. Kozawa, T. Kal Ki-Kis and J. F. Yeager, *J. Electrochem. Soc., 113* (1966) 405.
205 A. Kozawa, in S. Yashizawa *et al.* (eds.), *Electrochemistry of Manganese Dioxide and Manganese Dioxide Batteries in Japan*, Vol. 2, U.S. Branch Office, Electrochem. Soc. Jpn., Cleveland, OH, 1973, Chap. 3, pp. 39 - 64.
206 E. C. Muly and H. N. Frock, *MnO_2 Symp. Proc., Tokyo, 2* (1980) 251.
207 M. Sugimori, *MnO_2 Symp. Proc., Cleveland, OH, 1* (1975) 256.
208 A. Kozawa and R. A. Powers, *Electrochem. Technol., 5* (1967) 535.
209 G. S. Bell and R. Huber, *J. Electrochem. Soc., 111* (1964) 1.
210 W. Feitknecht, *Pure Appl. Chem., 9* (1964) 423.
211 N. Yamamoto, M. Kiyama and T. Takada, *Jpn. J. Appl. Phys., 12* (1973) 1827.
212 W. C. Maskell, J. A. E. Shaw and F. L. Tye, *Electrochim. Acta, 26* (1981) 1403.
213 C. Drotschmann, *Batterien, 17* (1963) 485.
214 R. Giovanoli, K. Bernhard and W. Feitknecht, *Helv. Chim. Acta, 51* (1968) 355.
215 R. Giovanoli and U. Leuenberger, *Helv. Chim. Acta, 52* (1969) 2333.
216 W. C. Maskell, J. A. E. Shaw and F. L. Tye, *J. Appl. Electrochem., 12* (1982) 101.
217 P. M. de Wolff, *Acta Crystallogr., 12* (1959) 341.
218 J. B. Fernandes, B. D. Desai and V. N. Kamat Dalal, *Electrochim. Acta, 29* (1984) 181.
219 S. B. Kanungo, K. M. Parida and B. R. Sant, *Electrochim. Acta, 26* (1981) 1147.
220 A. Kozawa, *MnO_2 Symp. Proc., Tokyo, 2* (1980) 321.
221 A. Kozawa, *Denki Kagaku, 44* (1976) 572.
222 L. Companella and G. Pistoia, *J. Electrochem. Soc., 118* (1971) 1905.
223 A. Kozawa and R. A. Powers, *J. Chem. Educ., 49* (1972) 587.
224 D. W. Murphy and P. A. Cristian, *Science, 205* (1979) 651.
225 R. S. Johnson and W. C. Vosburgh, *J. Electrochem. Soc., 100* (1953) 471.
226 K. Neumann and E. v. Roda, *Z. Elektrochem. Ber. Bunsenges. Phys. Chem., 69* (1965) 347.
227 S. Atlung, Paper presented at the I.S.E. Meeting, Div. 6, Kelkheim, 1973.
228 S. Atlung, *MnO_2 Symp. Proc., Cleveland, OH, 1* (1975) 47.
229 S. Atlung and T. Jacobsen, *Electrochim. Acta, 26* (1981) 1447.
230 W. C. Maskell, J. A. E. Shaw and F. L. Tye, *J. Power Sources 8* (1982) 113.
231 S. Atlung, personal communication.
232 W. C. Maskell, J. A. E. Shaw and F. L. Tye, *Electrochim. Acta, 27* (1982) 425.
233 W. C. Maskell, J. A. E. Shaw and F. L. Tye, *Electrochim. Acta, 28* (1983) 225.
234 W. C. Maskell, J. A. E. Shaw and F. L. Tye, *Electrochim. Acta, 28* (1983) 231.
235 E. Preisler, *MnO_2 Symp. Proc., Tokyo, 2* (1980) 184.
236 H. D. Holler and L. M. Ritchie, *Trans. Am. Electrochem. Soc., 37* (1920) 607.
237 F. Daniels, *Trans. Am. Electrochem. Soc., 53* (1928) 45.
238 B. M. Thompson, *Ind. Eng. Chem., 20* (1928) 1176.
239 K. Sasaki, *Mem. Fac. Eng. Nagoya Univ., 3* (1951) 81.
240 N. C. Cahoon, *J. Electrochem. Soc., 99* (1952) 343.
241 R. S. Johnson and W. C. Vosburgh, *J. Electrochem. Soc., 99* (1952) 317.
242 A. Kozawa, *J. Electrochem. Soc., 106* (1959) 552.
243 J. Muller, F. L. Tye and L. L. Wood, in D. H. Collins (ed.), *Batteries, 2*, Pergamon Press, Oxford, 1965, p. 201.
244 P. Benson, W. B. Price and F. L. Tye, *Electrochem. Technol., 5* (1967) 517.
245 A. Kozawa, *J. Electrochem. Soc., 106* (1959) 79.
246 J. Caudle, K. Summer and F. L. Tye, *J. Chem. Soc. Faraday Trans., 69* (1973) 876.
247 J. Caudle, K. Summer and F. L. Tye, *J. Chem. Soc. Faraday Trans., 69* (1973) 885.

248 A. Kozawa, *Extended Abstr., Electrochem. Soc., 15* (2) (1975) 27.
249 I. Tari and T. Hirai, *Electrochim. Acta, 26* (1981) 1657.
250 I. Tari and T. Hirai, *Electrochim. Acta, 27* (1982) 149.
251 I. Tari and T. Hirai, *Electrochim. Acta, 27* (1982) 235.
252 T. Hirai, I. Tari and T. Chzuku, *Kenkyu Hokoku Asahi Garas Kogyo Gijutsu Shoreikai, 38* (1981) 215.
253 N. C. Cahoon, *Trans. Electrochem. Soc., 92* (1947) 159.
254 R. Friess, *J. Am. Chem. Soc., 52* (1930) 3083.
255 H. P. McMurdie, D. N. Craig and G. W. Vinal, *Trans. Electrochem. Soc., 90* (1940) 509.
256 G. S. Bell, *Extended Abstr., Electrochem. Soc., 75*(2) (1975) 15.
257 B. Foussord, V. Dechenaux, P. Croissant and A. Hardy, in J. Thompson (ed.), *Power Sources 7*, Academic Press, London, 1979, p. 445.
258 F. L. Tye, in M. Barak (ed.), *Primary Batteries for Civilian Use: Electrochemical Power Sources*, Peter Peregrinus, London, 1980, p. 112.
259 K. Sasaki and T. Takahashi, *Electrochim. Acta, 1* (1959) 261.
260 Y. Uetani, T. Iwamura and Y. Ishikawa, *MnO_2 Symp. Proc., Tokyo, 2* (1980) 505.
261 J. J. Coleman, *Trans. Electrochem. Soc., 90* (1951) 545.
262 A. M. Chreitzberg, Jr. and W. C. Vosburgh, *J. Electrochem. Soc., 104* (1957) 1.
263 S. Yoshizawa, in K. Takashi *et al.*, *Electrochemistry of Manganese Dioxide and Manganese Dioxide Batteries*, Vol. 1, U.S. Branch Office, Electrochem. Soc. Jpn., Cleveland, OH, 1971, Chap. 1, pp. 7 - 56.
264 S. Yoshizawa, *MnO_2 Symp. Proc., Tokyo, 2* (1980) 1.
265 K. Shinoda, H. Ohta and A. Izumi, *MnO_2 Symp. Proc., Tokyo, 2* (1980) 162.
266 R. B. Rozelle and H. A. Swain, *Analyt. Chem., 47* (1975) 1135.
267 C. W. Jennings and W. C. Vosburgh, *J. Electrochem. Soc., 99* (1952) 309.
268 F. L. Tye, in M. Barak (ed.), *Primary Batteries for Civilian Use: Electrochemical Power Sources*, Peter Peregrinus, London, 1980, p. 120 - 121.
269 M. Sugimori, *MnO_2 Symp. Proc., Tokyo, 2* (1980) 443.
270 G. Kanoh, M. Takashima and M. Takaoka, *MnO_2 Symp. Proc., Tokyo, 2* (1980) 134.
271 A. Kozawa, *Denki Kagaku Oyobi Kogyo Butsuri Kagaku, 50* (1982) 763.
272 A. Kozawa, *Denki Kagaku, 25* (1957) 322.
273 A. Kozawa, *Denki Kagaku, 44* (1976) 508.
274 M. Voinov, *Electrochim. Acta, 27* (1982) 833.
275 J. J. Coleman, *Trans. Electrochem. Soc., 90* (1946) 545.
276 F. L. Tye, in M. Barak (ed.), *Primary Batteries for Civilian Use: Electrochemical Power Sources*, Peter Peregrinus, London, 1980, p. 117.
277 C. R. St. Claire-Smith, J. A. Lee and F. L. Tye, *MnO_2 Symp. Proc., Cleveland, OH, 1* (1975) 132.
278 *Am. Nat. Stand. C.18.1*, 1972.
279 *International Electrotechnical Commission, Publ. 86-1*, 4th edn., 1976, plus *Amendment No. 1*, 1978, and *86-2*, 4th edn., 1977, plus *Amendments No. 1*, 1978 and *No. 2*, 1979.
280 A. Ohta, J. Watanabe and R. Furumi, *MnO_2 Symp. Proc., Cleveland, OH, 1* (1975) 159.
281 Y. Uetani and T. Togo, *MnO_2 Symp. Proc., Cleveland, OH, 1* (1975) 183.
282 T. Tsuchida, *MnO_2 Symp. Proc., Cleveland, OH, 1* (1975) 230.
283 J. Brenet, P. C. Piquet and J. Y. Welsh, *MnO_2 Symp. Proc., Tokyo, 2* (1980) 214.
284 J. Y. Welsh and P. C. Picquet, *Prog. Batteries Sol. Cells, 2* (1979) 119.
285 H. C. Shah, *J. Electrochem. Soc. India, 30*(2) (1981) 173.
286 A. Kozawa and J. F. Yeager, *J. Electrochem. Soc., 112* (1965) 959.
287 R. H. W. Sieh, *Symp. on Manganese Dioxide for Dry Cells, Amsterdam, 1964*, pp. 20 - 37.
288 L. Balewski and J. Brenet, *Electrochem. Technol., 5* (1967) 527.
289 G. S. Bell and J. Baner, *Electrochim. Acta, 14* (1969) 453.

290 C. R. A. Clauss and H. E. L. G. Scheweigart, *J. Electrochem. Soc., 123* (1976).
291 T. Väland and J. Coleman, MnO_2 cathodes in H_2SO_4, *D.R.E.O. Invention No. 70-72*, 1972.
292 K. Appelt and H. Purol, *Electrochim. Acta, 1* (1956) 326.
293 F. Kornfeil, *J. Electrochem. Soc., 106* (1959) 1062.
294 K. Appelt and F. Forechi, *Electrochim. Acta, 8* (1963) 639.
295 A. Kozawa and R. A. Powers, *Electrochem. Technol., 5* (1967) 535.
296 S. S. Markov, G. A. Seryshev, N. M. Surova and N. V. Korelava, *Elektrokhimiya, 14* (1978) 1939.
297 M. Sugimori, *MnO_2 Symp. Proc., Cleveland, OH, 1* (1975) 256.
298 G. Kanoh, M. Takashima and M. Takaoka, *MnO_2 Symp. Proc., Tokyo, 2* (1980) 136.
299 A. Kozawa, *Prog. Batteries Sol. Cells, 2* (1979) 104.
300 H. Y. Kang and C. C. Liang, *J. Electrochem. Soc., 115* (1968) 6 - 10.
301 D. Boden, C. J. Venuto, D. Wisler and R. B. Wylie, *J. Electrochem. Soc., 115* (1968) 334.
302 T. Ohira and H. Ogawa, *Nat. Tech. Rep., 16* (1970) 209.
303 K. M. Miyazaki, in K. Takashi *et al.*, *Electrochemistry of Manganese Dioxide and Manganese Dioxide Batteries*, Vol. 2, U.S. Branch Office, Electrochem. Soc. Jpn., Cleveland, OH, 1971, pp. 123 - 153.
304 J. McBreen, *Electrochim. Acta, 20* (1975) 221.
305 K. Kordesch and J. Gsellmann, in J. Thompson (ed.), *Power Sources 7*, Academic Press, London, 1979, pp. 557 - 570.
306 K. Kordesch, J. Gsellmann, M. Peri, K. Tomantschger and R. Chemelli, *Electrochim. Acta, 25* (1981) pp. 1495 - 1504.
307 R. Chemelli, J. Gsellmann, G. Körbler and K. Kordesch, *Proc. Symp. MnO_2, Tokyo, 2* (1980) 153; *Extended Abstr.* 57 - 62, Electrochem. Soc. Jpn., 1980.
308 E. Voss and G. Huster, *Chem.-Ing.-Tech., 38* (1966) 623.
309 S. Suzuki, Y. Kanada, K. Takahashi, T. Shirogami and T. Takamura, *MnO_2 Symp. Proc., Cleveland, OH, 1* (1975) 402.
310 F. L. Tye, Plenary Lecture, *Electrochem. Soc. Symp. on MnO_2 Electrodes (Theory and Practice for Electrochemical Applications), New Orleans, Louisana, 10 - 12 October 1984.*
311 F. L. Tye, *Electrochim. Acta, 30* (1985) 17.